Synthesis, Characterization & Molecular Docking Studies of Thiazolidine Derivatives And Their Assessment As Potential Anti-Leishmanial Agents

Presented by: Raja Waleed Sajjad

CIIT/FALL-22-RPY-021/ATD

Supervisor: Dr. Yasser M.S.A. Alkahraman

Co-Supervisor: Dr. Muhammad Hasham Bin Asad

Contents

- Introduction
- Aims and Objectives
- Statement Problem
- Research Methodology
- Results
- Discussions
- Conclusion
- Future Prospective
- Acknowledgment
- References

Introduction of Leishmania

Leishmaniasis is a parasitic disease caused by the leishmanian protozoa genus spread to human beings by bite of sandfly phlebotomine, more than 30 different species of phlebotomine sandfly transfer parasite to human.

In Pakistan, leishmaniasis is an endemic disease, particularly prevalent in the regions of Khyber Pakhtunkhwa, Baluchistan, and parts of Sindh. The country experiences a high burden of cutaneous leishmaniasis, with outbreaks frequently reported. The first documented case of leishmaniasis in Pakistan dates back to the early 20th century. Over the years, the disease has become a significant public health concern, with thousands of new cases reported annually.

(Legrand et al., 2021;kayani et al., 2021)

Transmission and Life Cycle

Transmitted by the bite of infected female sandflies, the parasite undergoes a life cycle between the sandfly vector and mammalian hosts.

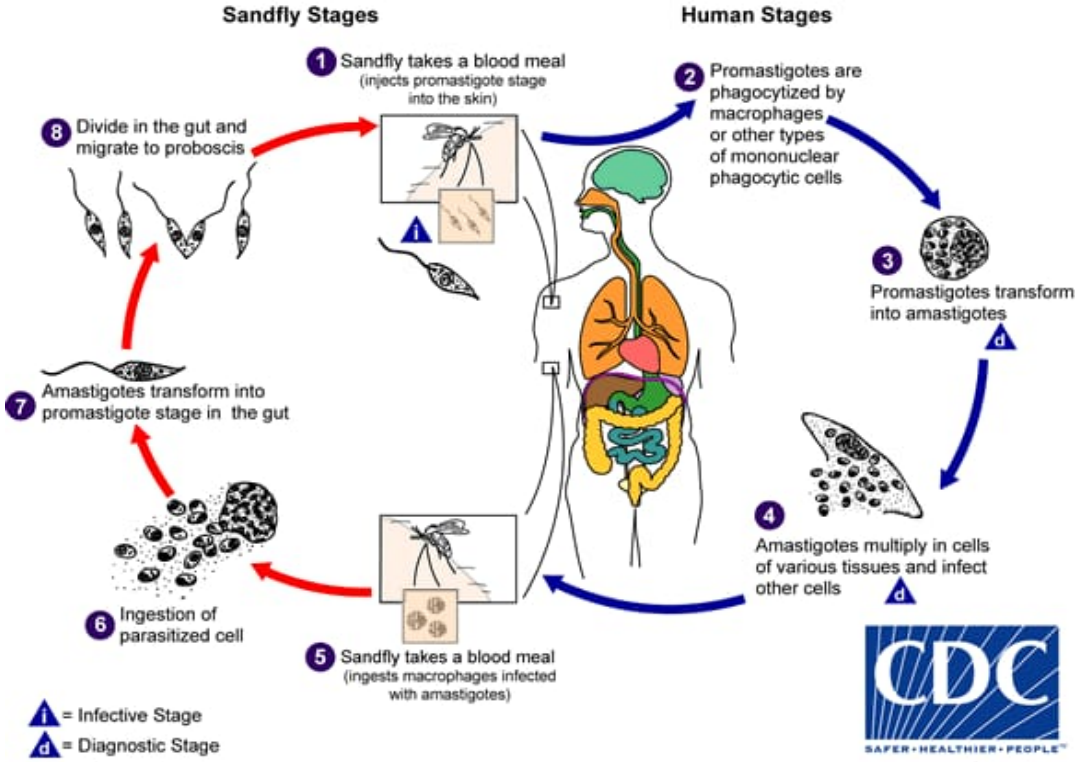

(Alvar et al., 2012)

Types of Leishmania and Enzyme Targets

Leishmania, a parasitic disease affecting humans, is primarily caused by three main species: *Leishmania donovani*, which leads to *visceral leishmaniasis*; *Leishmania tropica*, responsible for *cutaneous leishmaniasis*; and *Leishmania braziliensis*, which causes *mucocutaneous leishmaniasis*.

The survival and proliferation of these parasites depend heavily on several vital enzymes. Dihydrofolate Reductase (DHFR) is essential for DNA synthesis and cell replication, while Trypanothione Reductase plays a crucial role in maintaining redox balance within the parasite. Additionally, Glutathione Reductase (GR) is important for detoxifying reactive oxygen species, and Glyceraldehyde-3-Phosphate Dehydrogenase (GAPDH) is a key enzyme in glycolysis, vital for energy production. Inhibiting these enzymes disrupts critical biological pathways, leading to the death of the parasite, making them effective drug targets for treating leishmaniasis.

(Goto et al., 2018)

Current Treatments

Current treatments for leishmaniasis include several drugs, each with significant limitations. Antimonials are the first-line treatment but are associated with high toxicity and resistance issues. Amphotericin B is effective but comes with severe side effects and high costs. Miltefosine, an oral drug, faces challenges of emerging resistance and teratogenic risks. The disadvantages of these current treatments include high toxicity, prolonged treatment durations, resistance development, and expensive treatment costs.

In contrast, thiazolidine derivatives offer several advantages. They exhibit strong binding affinity to Leishmania enzymes, reduced toxicity, potential to overcome resistance, and lower costs. Thiazolidine derivatives show promise as safer and more effective treatment options for leishmaniasis.

(Lindoso et al., 2010)

General Inhibitors for Leishmaniasis

Variety of Analogs/Inhibitors belonging to different classes of compounds have been used for the study of leishmaniasis. i.e. Pyrimidines, Quinazoline, Thiosemicarbazones, Chalcones etc.

The scheme for the proposed study is synthesis of thiazolidine derivatives as leishmania inhibitors.

Thiazolidine Derivatives

Thiazolidine is a five-membered ring structure that includes both sulfur and nitrogen atoms. It is formed by the reaction of a thiol (-SH) and an amine (-NH) with an aldehyde or ketone. This ring structure is key to the compound's stability and reactivity. The sulfur atom enhances the binding affinity to biological targets, while the nitrogen atom improves hydrogen bonding and drug solubility. These characteristics are crucial for its anti-leishmanial activity.

Thiazolidine derivatives exhibit strong interactions with enzymes such as Trypanothione Reductase and GAPDH, which are vital for the parasite's survival. Additionally, the stability and bioavailability of these derivatives make them effective therapeutic candidates, offering potential advantages over current treatments.

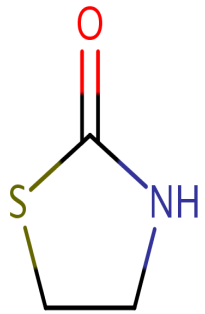

(Chaudhry et al., 2022)

Pharmacological Importance Of Thiazolidine
Anti-Leishmanial Activity

Thiazolidine derivatives have demonstrated significant anti-leishmanial activity, effectively targeting and inhibiting the growth of Leishmania parasites. These compounds interfere with the parasite's metabolic pathways, providing a promising approach for treating leishmaniasis. Their chemical diversity allows for the development of potent anti-leishmanial therapies.

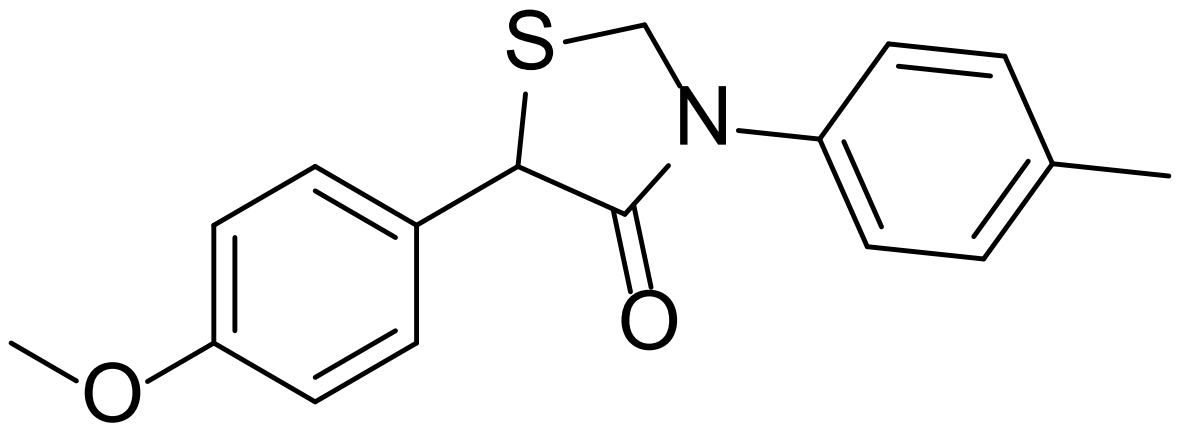

(Manjula et al., 2009)

Anti leishmanial Activity

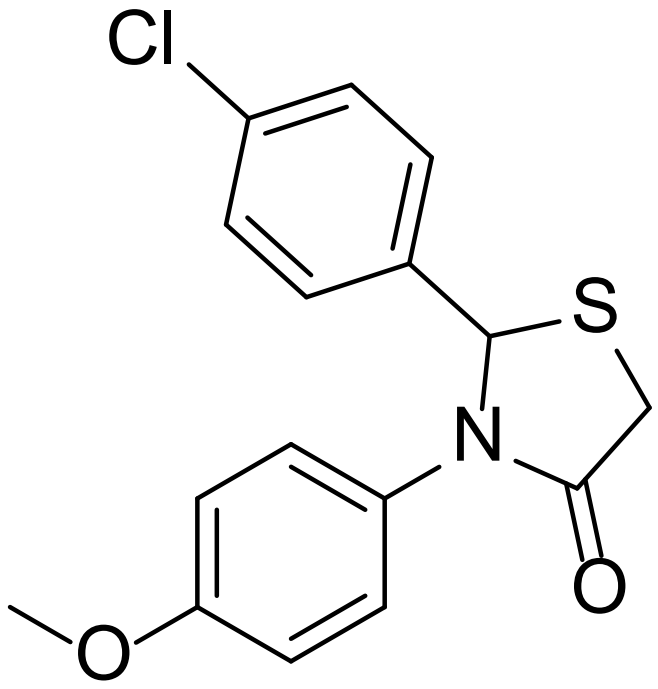

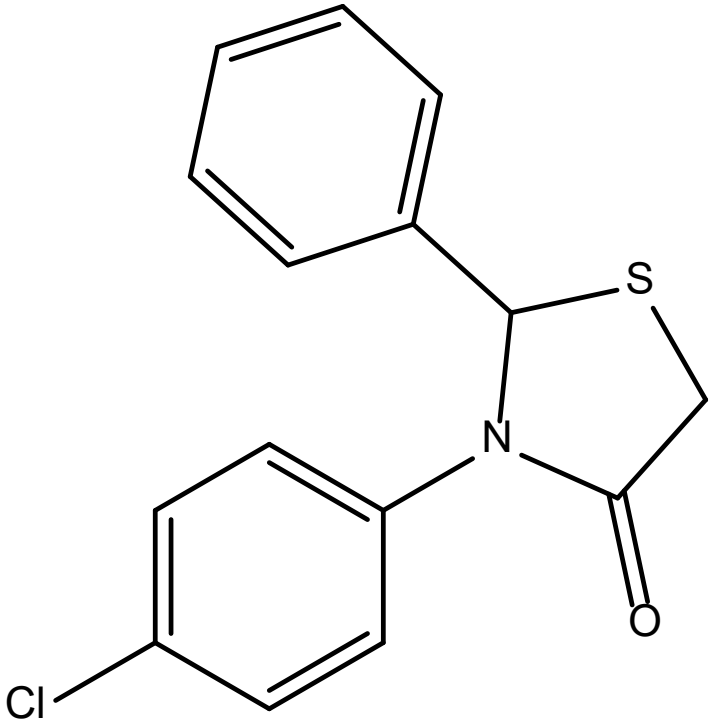

(Gupta et al., 2009)

Anti Diabetic Activity

Thiazolidine derivatives, particularly thiazolidinediones, are widely used as anti-diabetic agents to improve insulin sensitivity and glucose metabolism. They activate PPAR-γ receptors, enhancing insulin response and reducing blood sugar levels. This makes them essential in managing type 2 diabetes mellitus.

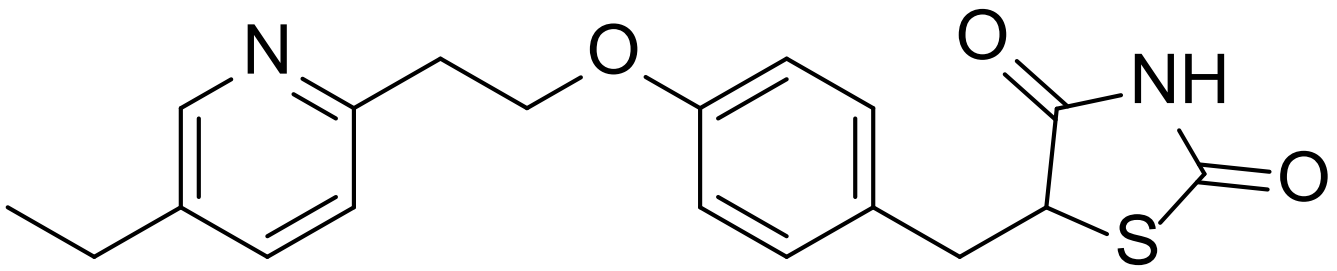

Structure of Pioglitazone

(Hou et al., 2023)

Anti Microbial Activity

Thiazolidine compounds are significant in anti-microbial research due to their broad-spectrum activity against bacteria and fungi.

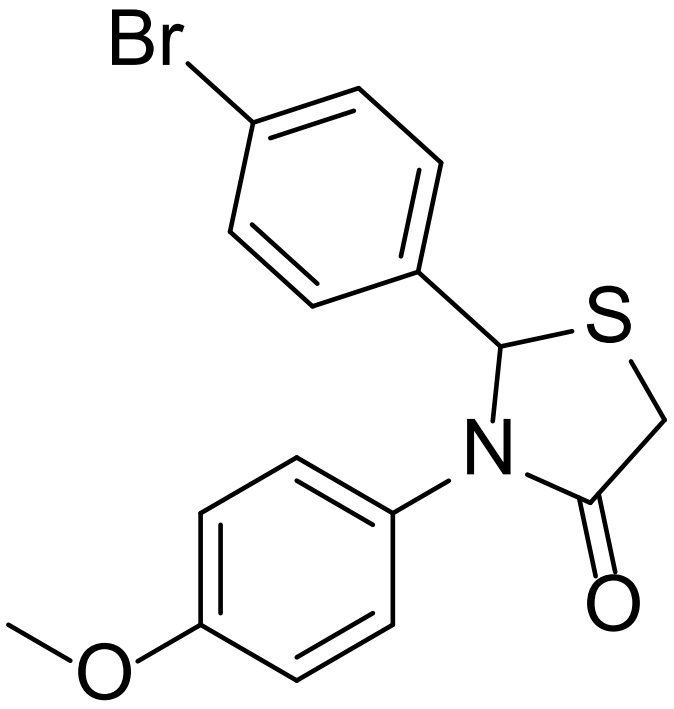

(Manjula et al., 2023)

Statement Of the Problem

A variety of scaffolds have been reported in the literature as lead structures to be antileishmanial agents. However, mostly these lead compounds have been identified through trial-and-error methodology and possess many side effects and a history of toxicities.

Thiazolidine derivatives antileishmanial compounds targeting *in silico* of Glyceraldehyde 3-phosphate dehydrogenase enzyme (GADPH) & trypanothione Reductase (TR) enzyme & Glutathione Reductase Enzyme (GR) have not been Signature for leishmaniasis.

The thiazolidine functional group in thiazolidine derivatives is crucial for disrupting *Leishmania* enzymes like Glyceraldehyde 3-phosphate dehydrogenase enzyme (GADPH) and trypanothione reductase due to its structural interactions with the enzyme's active sites, thereby disrupting essential metabolic pathways. Therefore, there is a strong need to search for alternative inhibitors to treat leishmaniasis.

Aims And Objectives

The objective is to create and analyze a fresh set of Thiazolidine derivatives while assessing their potential as anti-leishmanial agents.

1. To synthesize Thiazolidine analogue.
2. To characterize the synthesized derivatives using spectroscopic techniques.
3. To conduct *In vitro* studies (Promastigotes studies of L. Major *Leishmania* tropica).
4. To conduct *In-Silico* studies of Trypanothione reductase, Glutathione Reductase (GR) & Glyceraldehyde 3-phosphate dehydrogenase (GAPDH).

Research Methodology

- Synthesis of Thiazolidine Derivatives
- Characterization using NMR, and FTIR
- *In vitro* Promastigotes/Amastigotes Assay
- hDHFR Enzymes Assay
- *In silico* studies

Synthesis Of Thiazolidine derivatives
General scheme of synthesis

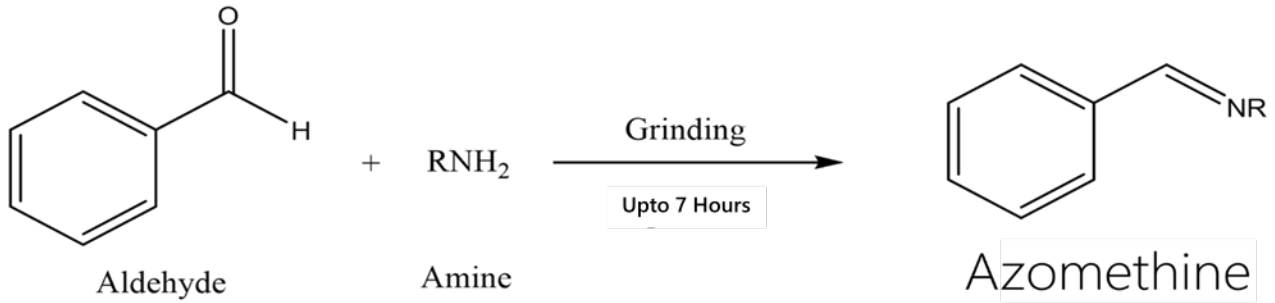

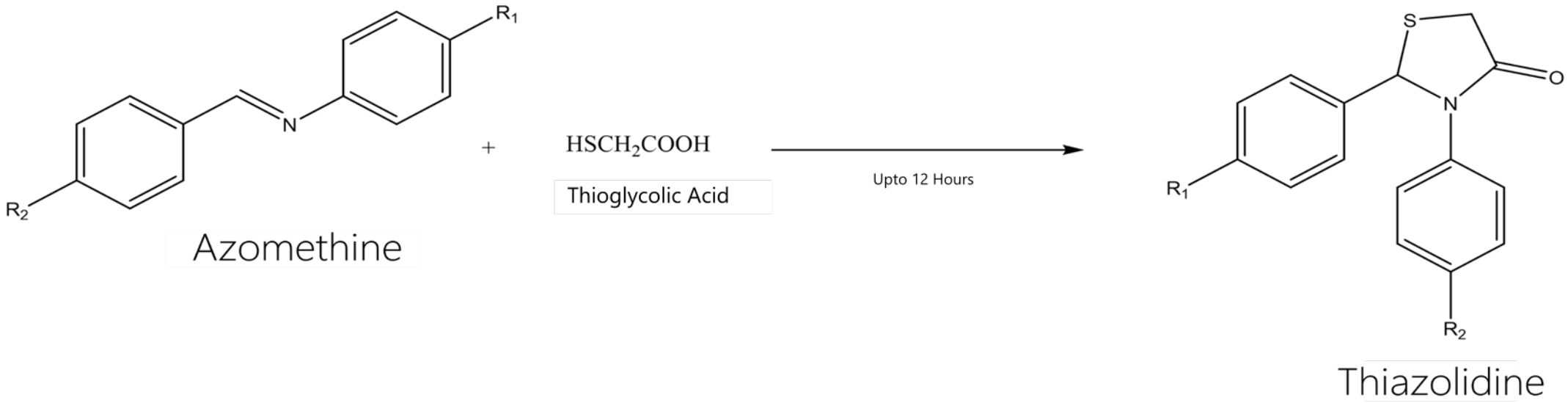

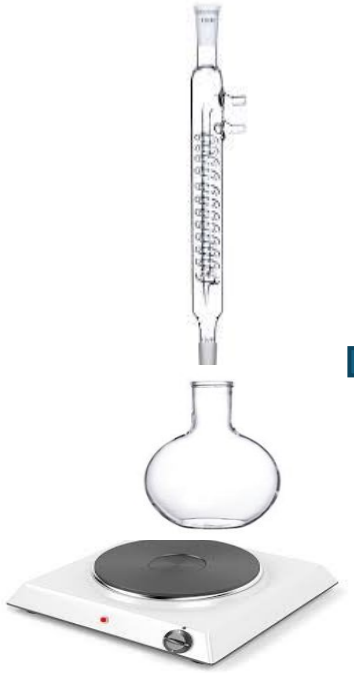

(Aldehyde + Amine)

Reflux

Up to 7 Hour

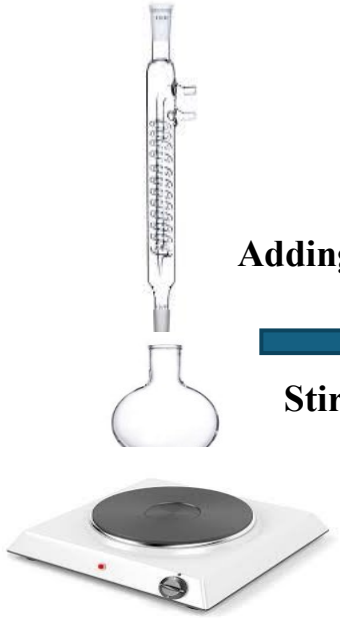

(Azomethine)

Adding H_2SO_4

Stir for one hour at r.t

Thiaglycolic Acid

Reflux at 110c

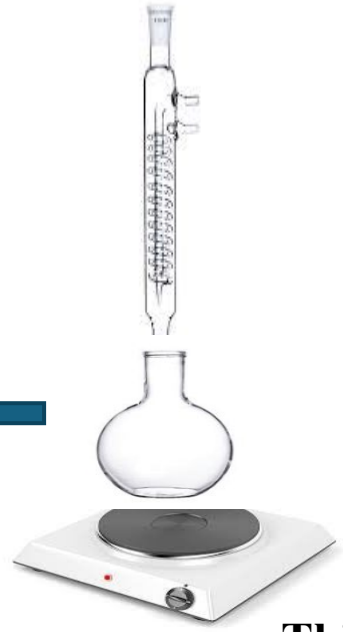

Thiazolidine

Filtration

purification

Drying

Methodology of Synthesis

Ten millimoles each of an aldehyde and an amine were individually weighed and dissolved in separate beakers containing 20 mL of anhydrous ethanol, aided by gentle heating and stirring on a magnetic stirrer until complete dissolution. The solutions were then combined in a round-bottomed flask equipped for reflux, including a condenser and Dean-Stark trap.

The mixture was heated to 78°C, the boiling point of ethanol, with continuous temperature monitoring. Small aliquots were periodically withdrawn and analyzed using thin-layer chromatography (TLC) against a reference sample to monitor the reaction progress, which typically took approximately 7 hours to yield the desired Schiff base. After confirming completion, the reaction mixture was cooled, and ethanol was evaporated overnight. The resulting crude product was filtered and washed with solvents such as ethanol, methanol, and ethyl acetate to remove impurities. Characterization of the purified product was achieved using nuclear magnetic resonance (NMR), Fourier-transform infrared spectroscopy (FTIR), and melting point determination to confirm its identity as the desired Schiff base.

Ten millimoles of Schiff base were dissolved in 30 mL of toluene using a magnetic stirrer after gentle heating to ensure complete dissolution. Separately, 10.25 mmol of thioglycolic acid was dissolved in another 30 mL of toluene using the same method. The solutions were combined in a round-bottom flask equipped with a magnetic stirrer, condenser, and Dean-Stark trap, and heated to 110°C, monitored with a thermometer attached to the condenser. Thin-layer chromatography (TLC) using an ethyl acetate and n-hexane solvent system (1:3 ratio) was employed to monitor the reaction progress, with samples withdrawn every two hours and compared against a reference of starting materials.

Refluxing continued for about 12 hours until TLC confirmed product formation. After cooling, the mixture was washed with sodium bicarbonate solution and brine, and the organic layer was dried with anhydrous sodium sulfate, followed by solvent removal via rotary evaporation. Column chromatography and recrystallization from ethanol purified the product, verified by nuclear magnetic resonance (NMR), Fourier-transform infrared spectroscopy (FTIR), and melting point determination, demonstrating successful synthesis and characterization of the Schiff base-thioglycolic acid adduct.

- **Synthesis Of RWS-1**

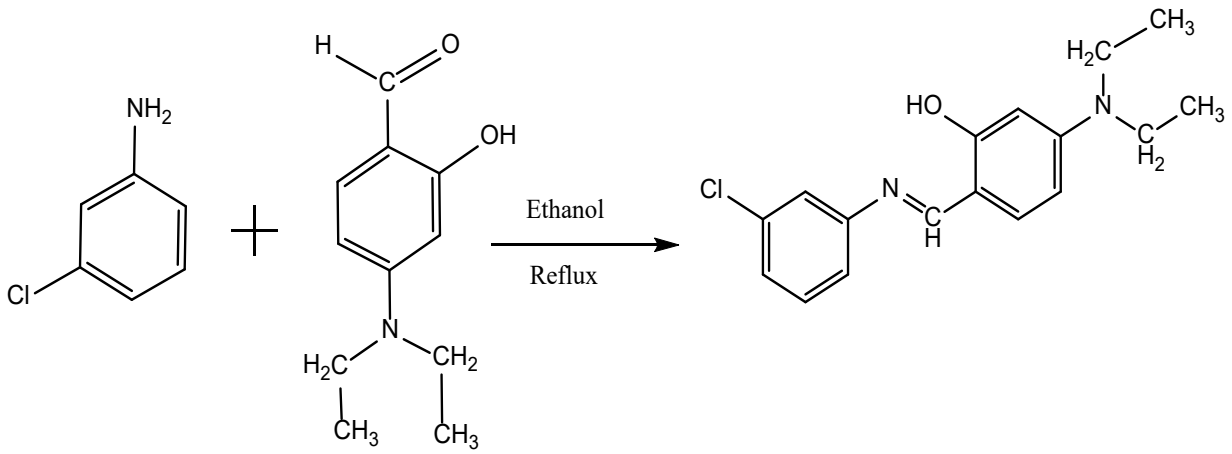

- **Synthesis Of RWS-3**

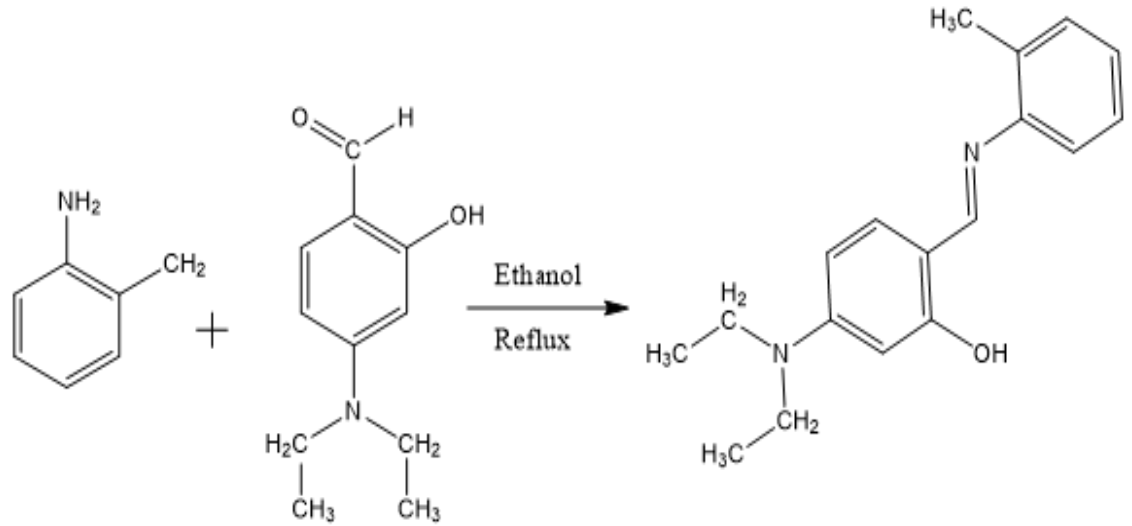

- **Synthesis Of RWS-2**

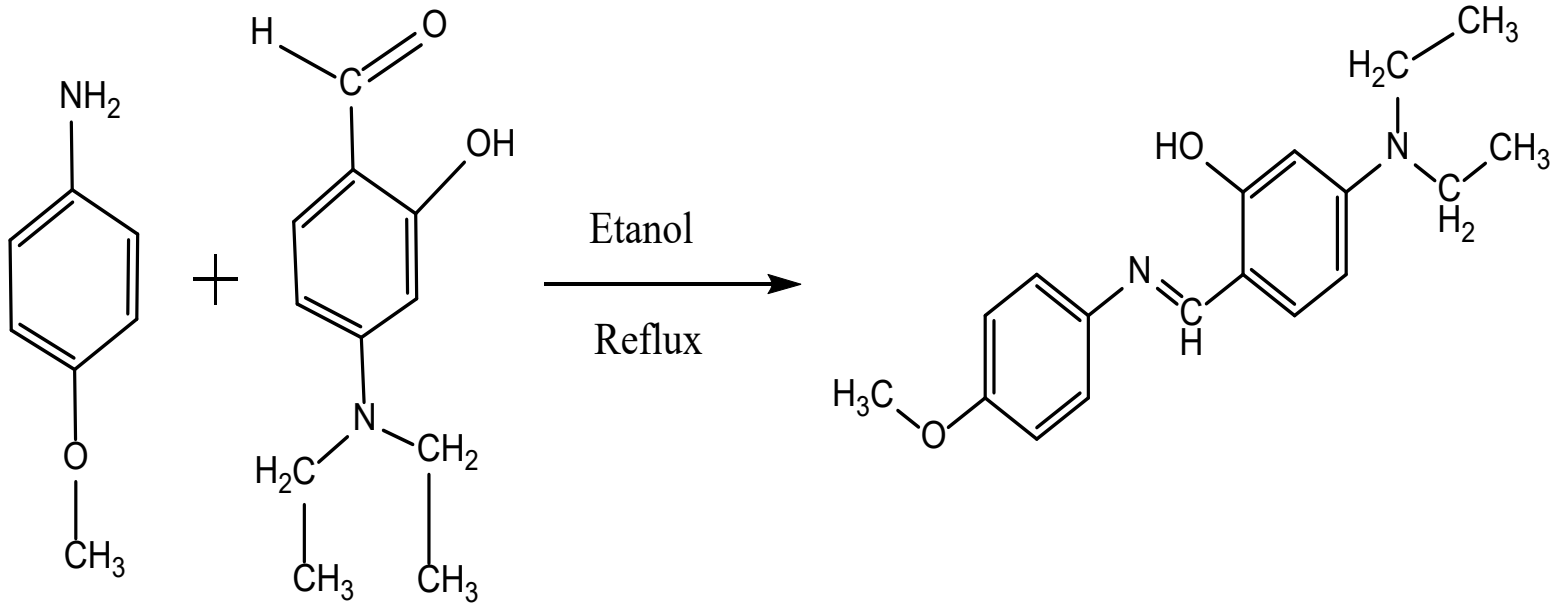

- **Synthesis Of RWS-4**

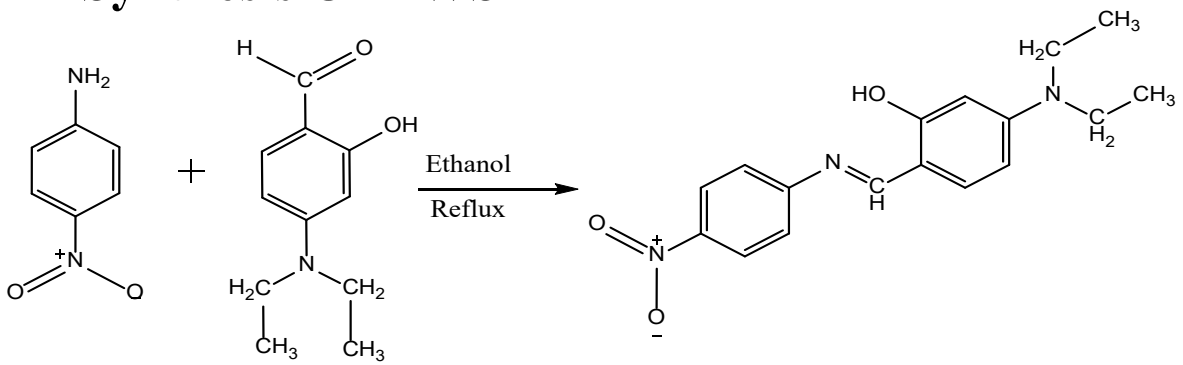

- **Synthesis Of RWS-6**

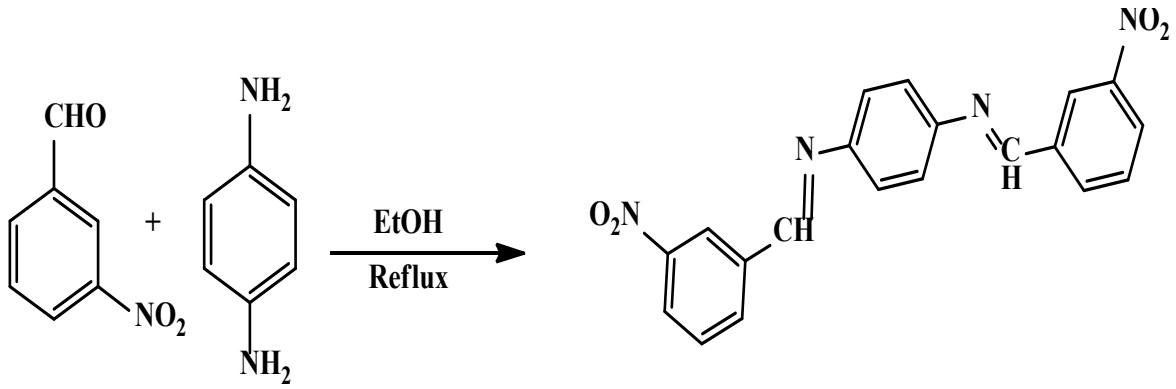

- **Synthesis Of RWS-5**

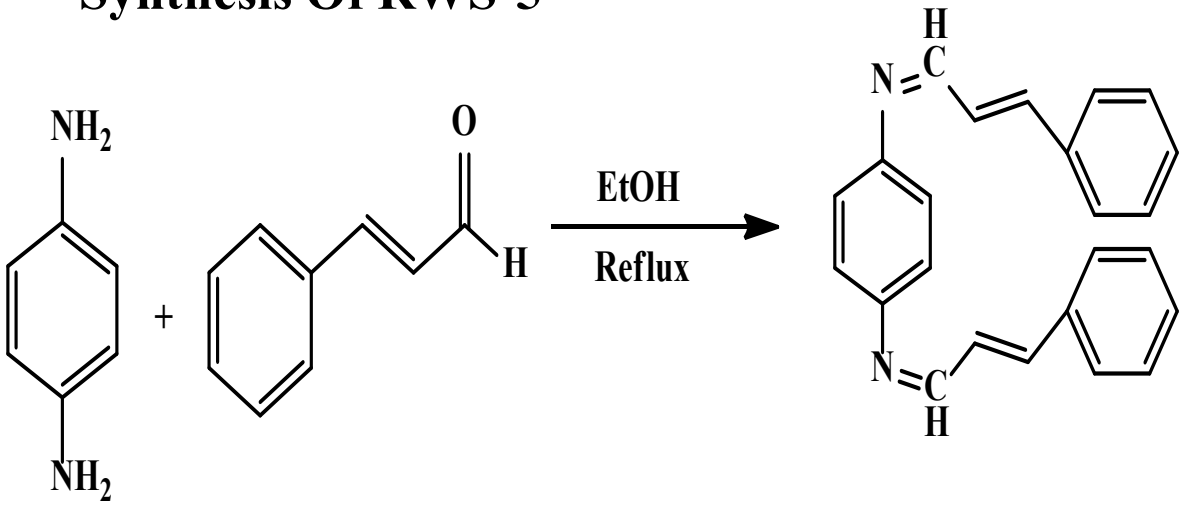

- **Synthesis Of RWS-7**

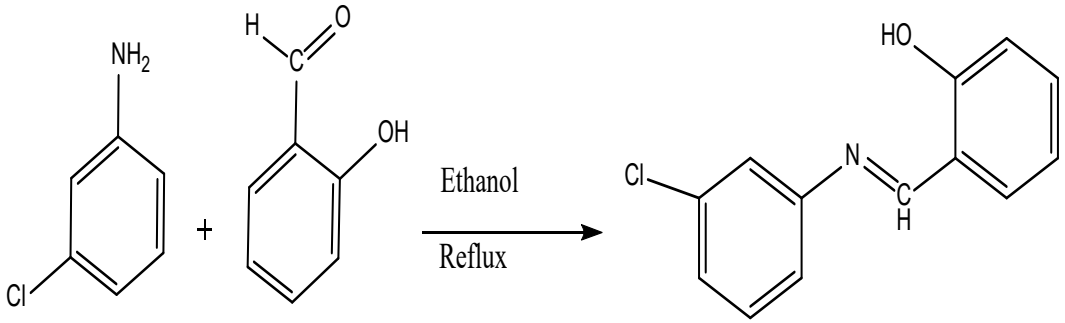

- **Synthesis Of RWT-1**

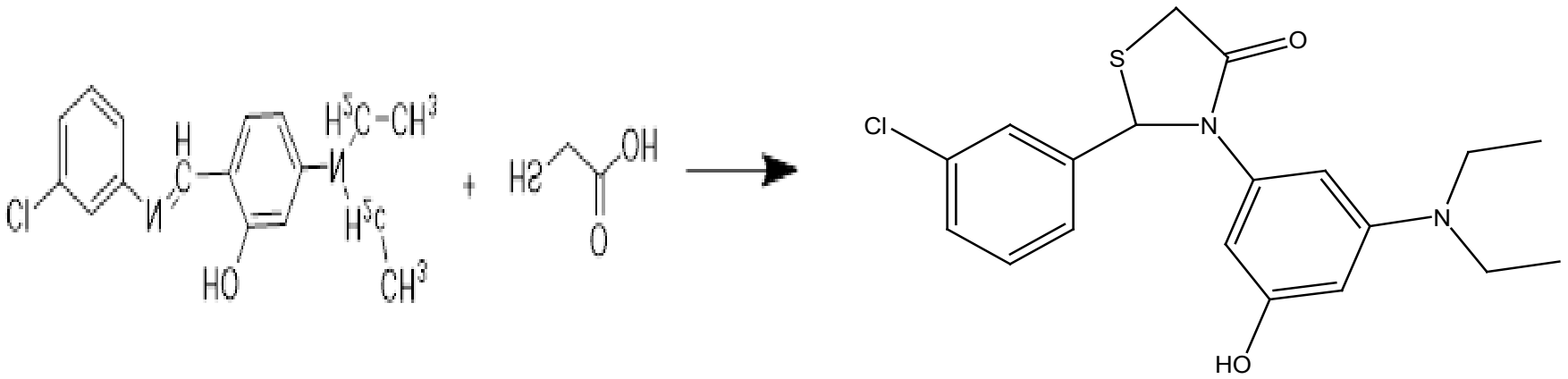

2-(3-chlorophenyl)-3-(3-(diethylamino)-5-hydroxyphenyl)thiazolidin-4-one

- **Synthesis Of RWT-2**

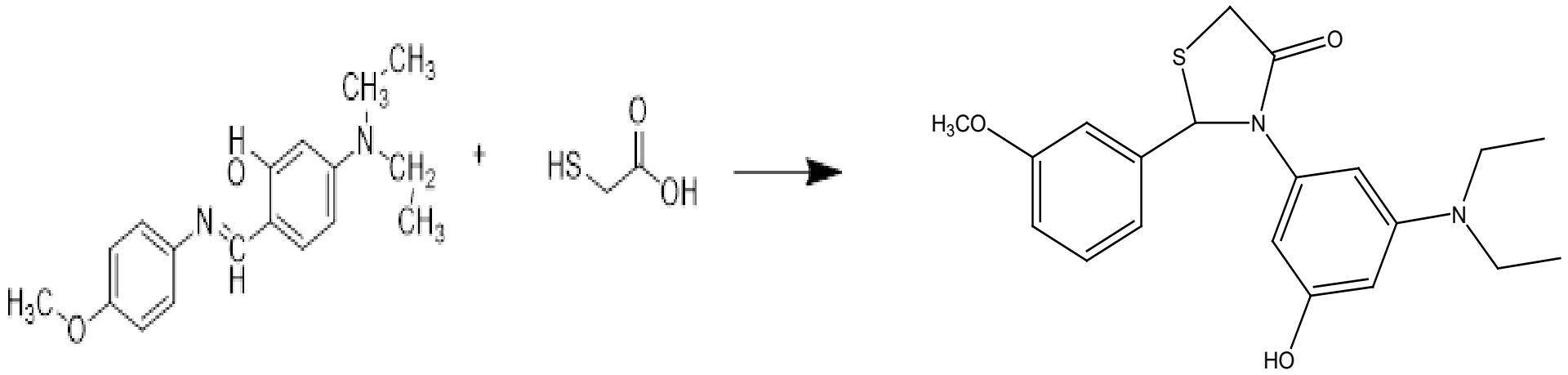

3-(3-(diethylamino)-5-hydroxyphenyl)-2-(3-methoxyphenyl)thiazolidin-4-one

- **Synthesis of RWT-3**

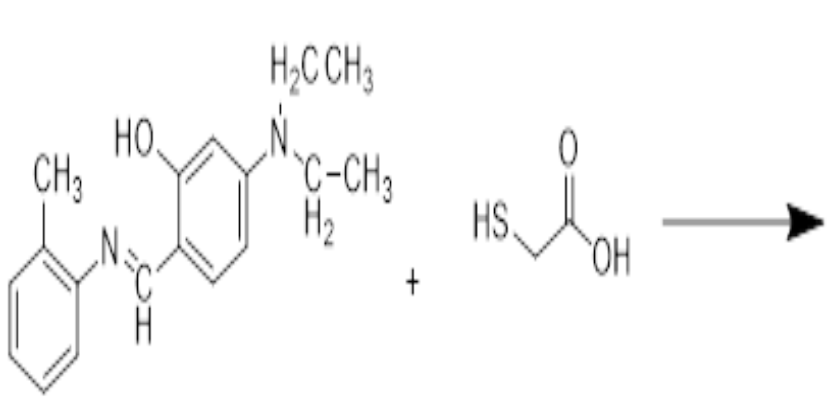

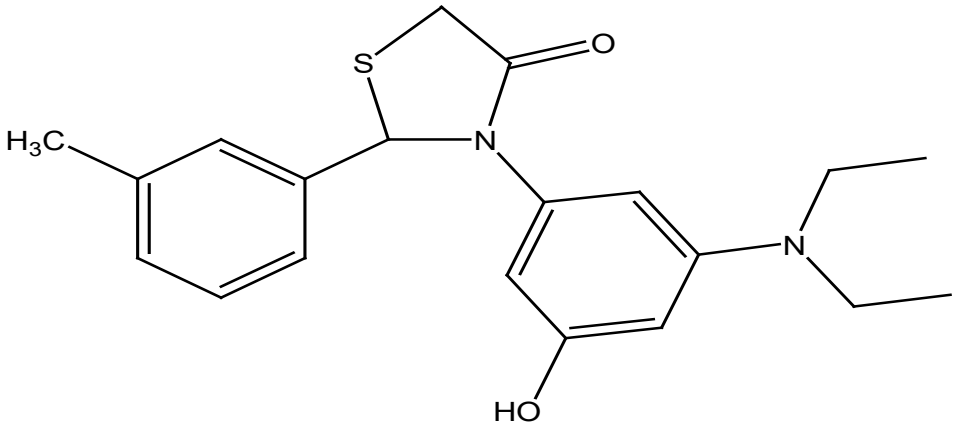

3-(3-(diethylamino)-5-hydroxyphenyl)-2-*m*-tolylthiazolidin-4-one

- **Synthesis of RWT-4**

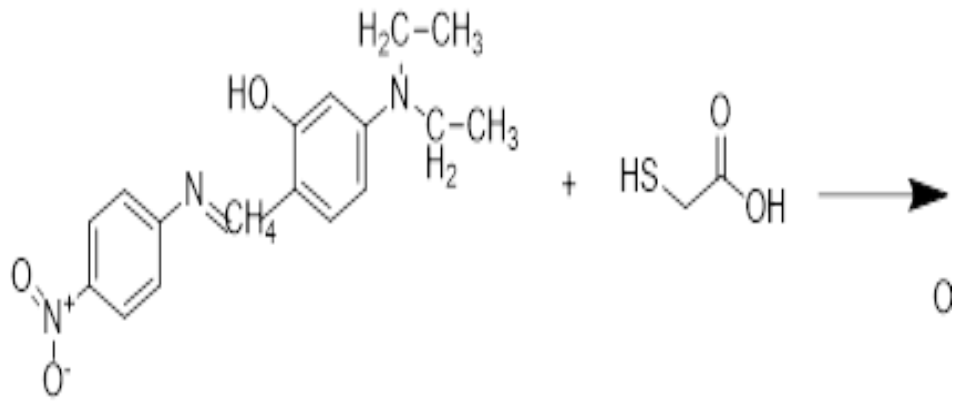

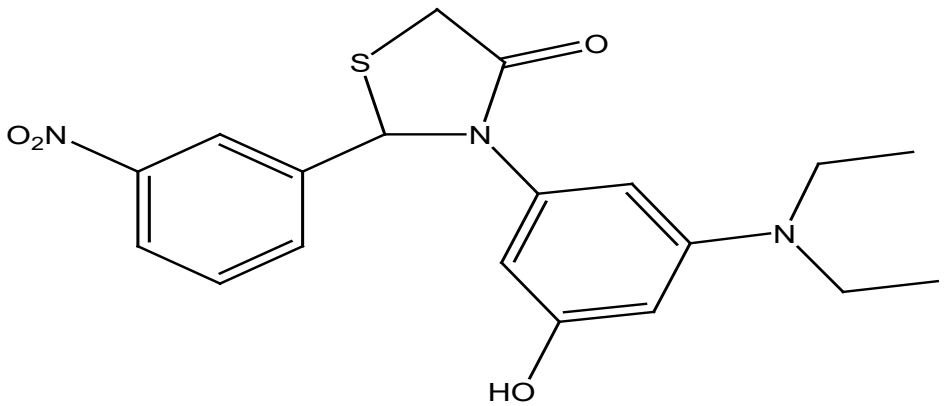

3-(3-(diethylamino)-5-hydroxyphenyl)-2-(3-nitrophenyl)thiazolidin-4-one

Characterization of the compounds

➢ **Chemical characterization**

The synthesized derivatives will be chemically characterized using

- NMR (Nuclear Magnetic resonance) and
- FTIR (Fourier- transform infrared)

➢ **Physical properties**

- Melting point
- Color
- Solubility
- % yield
- MW

Promastigotes Assay

To evaluate the anti-leishmanial activity of test compounds, Leishmania promastigotes are cultivated in RPMI-1640 medium supplemented with 10% fetal bovine serum (FBS) at 26°C. Parasites are harvested during their logarithmic growth phase, typically on day 3 or 4. For the assay setup, the parasite density is adjusted to 1×1061×10 6 cells/mL, and 100 µL of this suspension is dispensed into each well of a 96-well plate. Subsequently, 100 µL of test compounds at various concentrations are added to the wells, with amphotericin B serving as the positive control and DMSO as the negative control. The plates are then incubated at 26°C for 72 hours.

To assess parasite viability, 10 µL of MTT solution (5 mg/mL) is added to each well, followed by a 4-hour incubation at 26°C. After this period, 100 µL of DMSO is added to solubilize the formazan crystals formed. The absorbance is measured at 570 nm using a microplate reader, which provides an indication of cell viability based on metabolic activity.

(Spath et al., 2021)

Amastigotes Assay

To prepare for evaluating the anti-leishmanial activity of test compounds, human macrophages (e.g., THP-1 cells) are cultured in RPMI-1640 medium with 10% fetal bovine serum (FBS). These macrophages are differentiated using PMA (50 ng/mL) for 48 hours. For the infection step, the macrophages are infected with Leishmania promastigotes at a parasite-to-cell ratio of 10:1 and incubated for 24 hours to allow internalization and transformation into amastigotes. After infection, the cells are washed to remove extracellular parasites, and various concentrations of the test compounds are added, with miltefosine serving as the positive control and DMSO as the negative control. The infected macrophages are incubated with the compounds for 72 hours at 37°C in a 5% CO2 atmosphere.

To assess viability, the macrophages are lysed with 0.1% SDS to release the amastigotes, and the number of viable amastigotes is counted using a hemocytometer or Giemsa staining. Alternatively, a colorimetric assay, such as Alamar Blue, can be used to evaluate viability.

(Garraway et al., 2021)

DHFR Enzyme Assay

The assay for evaluating DHFR enzyme inhibition involves several critical steps to assess the effectiveness of test compounds. Initially, the DHFR enzyme is acquired either commercially or through recombinant expression. Substrate solutions of dihydrofolate (DHF) and NADPH are prepared and added to an assay buffer containing Tris-HCl, NaCl, and MgCl2 to create optimal enzymatic conditions. In a 96-well plate setup, the assay begins by adding DHF and NADPH solutions followed by test compounds at varying concentrations, along with positive (methotrexate) and negative (DMSO) controls.After setting up the plate, the enzyme reaction is initiated by introducing DHFR enzyme solution, resulting in a final concentration of 10 nM per well.

The mixture is gently mixed and allowed to incubate at 25°C for 30 minutes to facilitate enzymatic reactions. Following incubation, enzyme activity is assessed by monitoring absorbance changes over time, reflecting the rate of product formation. Comparison of enzyme activity in the presence of test compounds against controls enables the determination of inhibition levels, offering insights into the compounds' potential as DHFR enzyme inhibitors for therapeutic development.

(Frank et al., 2015)

Schematic flow chart

M199 media

Add Supplements

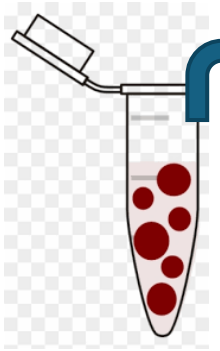

Promastigotes in Media

180uL/ Well

Drug sample

20uL/ Well

96 wells plate

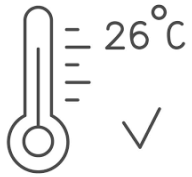

72

Reader

EC 50 Calculations

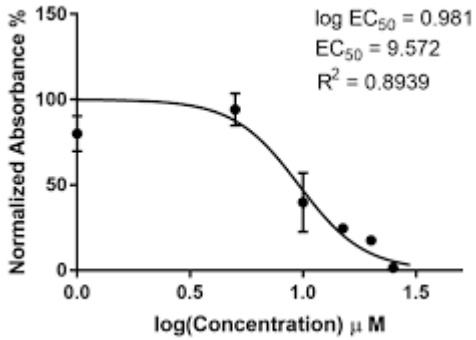

In Silico Studies

Molecular docking studies employing AutoDock Vina and Discovery Studio are integral to identifying effective treatments for Leishmania infections. These simulations predict how compounds interact with essential enzymes like DHFR, Trypanothione Reductase, GR, and GAPDH at a molecular level, guiding the development of potent drugs with specific binding capabilities and reduced resistance risks.In silico pharmacokinetic evaluations using Swiss ADME and LabWare software assess the ADME properties of potential drugs, optimizing their bioavailability and determining suitable dosing strategies in animal models.

Concurrently, toxicology assessments conducted with Tox-21 and LabWare software evaluate the safety profiles of these compounds, ensuring they meet regulatory standards and are safe for further clinical development. These computational approaches accelerate drug discovery and development processes, offering insights crucial for advancing effective therapies against leishmaniasis.

Results

- Physical characterization
- Structural analysis of synthesized compounds by using NMR & FTIR
- Anti amastigotes and Anti promastigotes Assays
- DHFR enzyme's assay
- Molecular docking studies
- *In silico* Pharmacokinetic studies
- *In silico* Toxicology studies

Physical Characteristics

Sr. No	Molecular Weight (g/mol)	Molecular Formula	Physical Appearance	Color	Melting Point (°C)	Yield (%)
RWS-1	302	$C_{17}H_{19}ClN_2O$	Crystals	Yellow	135	98
RWS-2	298	$C_{18}H_{22}N_2O_2$	Grains	Yellow	117	87
RWS-3	282	$C_{19}H_{22}N_2O_2$	Powder	Brown	145	85
RWS-4	314	$C_{17}H_{20}N_3O_3$	Crystals	Red	190	77
RWS-5	336.43	$C_{24}H_{20}N_2$	Crystals	Yellow	225	70
RWS-6	374.35	$C_{20}H_{14}N_4O_4$	Powder	Brown	210	90
RWS-7	231	$C_{13}H_{10}ClNO$	Powder	Yellow	116	94
RWT-1	362	$C_{18}H_{19}ClN_2O_2S$	Crystals	Yellow	143	85
RWT-2	358	$C_{19}H_{22}N_2O_3S$	Grains	Yellow	130	90
RWT-3	342	$C_{19}H_{22}N_2O_2S$	Powder	Light Brown	155	76
RWT-4	374	$C_{19}H_{22}N_2O_3S$	Crystals	Red	195	85

FTIR Analysis of Compounds

- **RWS-1**

FTIR (Vmax, cm-1): 3415 (br, O-H), 2915 (C-H), 1617 (C=N), 1450 (C=C), 1219 (C-N), 1137 (C-O), 845 (C-Cl)

- **RWS-2**

FTIR (Vmax, cm-1): 3450 (O-H), 3100-2850 (C-H), 1593 (C=N), 1496 (C=C), 1270 (C-N), 1066 (C-O)

- **RWS-3**

FTIR (Vmax, cm-1): 3510-3280 (br, O-H), 2968 (C-H), 1596(C=N), 1520 (C=C), 1339 (C-N), 1128 (C-O)

- **RWS-4**

FTIR (Vmax, cm-1) 3460 (O-H), 3068(C-H), 1610 (C=N), 1521, 1300 (NO_2), 1349 (C-N)

FTIR Analysis of Compounds (continued)

- **RWS-5**

FT-IR (Vmax, cm-1): 3088(Ar C-H), 3024(C-H), 1621(C=N), 1580(C=C)

- **RWS-6**

FT-IR (Vmax, cm-1): 3059(C-H), 1625(C=N), 1521,1300(N02), 1349(C-N)

- **RWS-7**

FTIR (Vmax, cm-1): 3500(N-H), 3100(O-H), 1613(C=N), 1566 (C=C), 1278 (C-N), 1184(C-O), 751(C-Cl)

FTIR Analysis of Compounds (continued)

- **RWT-1**

FTIR (Vmax, cm-1): 3450 (br, O-H), 3370 (N-H), 3063 (C-H), 1650 (C=O), 1490 (C=C), 1320 (C-N), 1217 (C-O), 722 (C-Cl)

- **RWT-2**

FTIR (Vmax, cm-1): 3430 (O-H), 3230 (N-H), 2930 (C-H), 1660 (C=O), 1505 (C=C), 1296 (C-N), 1120 (C-O)

- **RWT-3**

FTIR (Vmax, cm-1): 3437 (O-H), 3331 (N-H), 3037 (C-H), 1650 (C=O), 1530 (C=C), 1320 (C-N), 1128 (C-O)

- **RWT-4**

FTIR (Vmax, cm-1): 3350 (O-H), 3230 (N-H), 3050-2900 (C-H), 1650 (C=O), 1570 (C=C), 1550, 1350, NO2, 1260 (C-N)

STRUCTURAL ANALYSIS OF COMPOUNDS (RWS-1 and RWS-2)

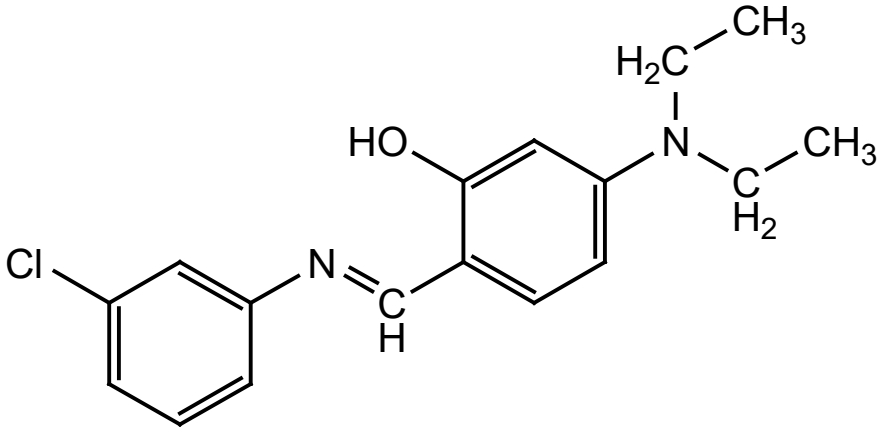

1H-NMR (DMSO-d6, 300 MHz), chemical shift (ppm): 8.28 (s, 1H), 7.34 (m, 5H), 6.77 (br, s, 1H), 6.39 (d, J = 8.7 Hz 1H), 5.59 (s, 1H), 3.87 (q, J = 6.9 Hz, 4H), 1.25 (t, J = 7.2 Hz, 6H)

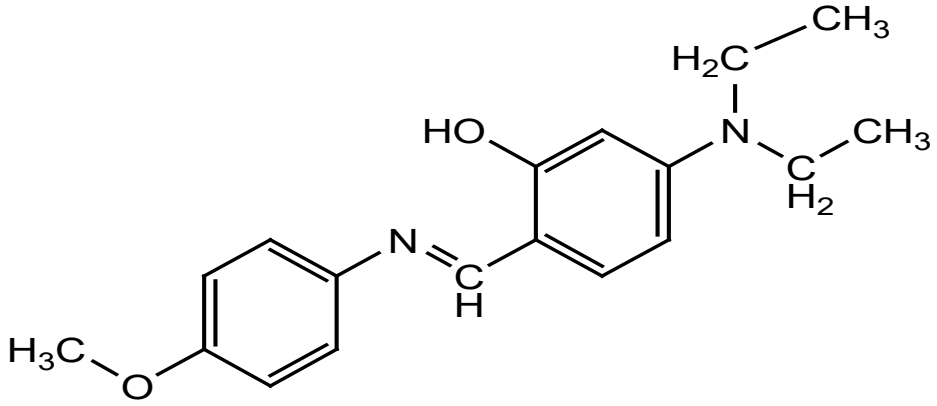

H-NMR (DMSO-d6, 300 MHz), chemical shift (ppm): 8.38 (s, 1H), 7.25(m, 4H), 6.99 (8.7, 2H), 6.51 (br, s, 1H), 6.38 (dd, J = 9, 2.4 Hz 1H), 3.98 (s, 3H), 3.49 (q, J = 7.2 Hz, 4H), 1.26 (t, J = 7.2 Hz, 6H)

STRUCTURAL ANALYSIS OF COMPOUNDS (RWS-3 and RWS-4)

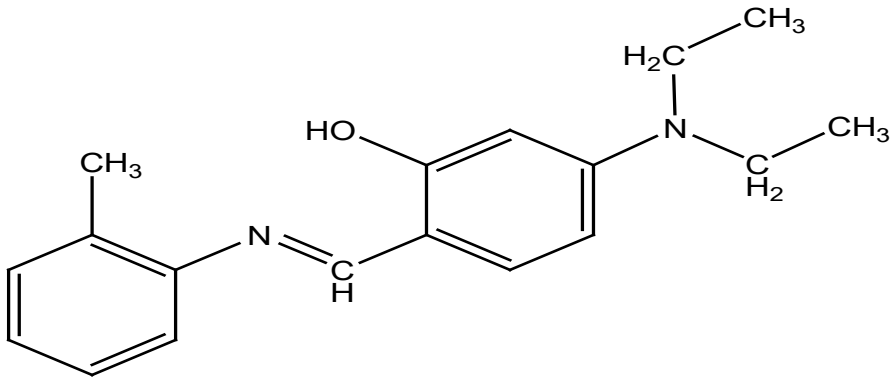

1H-NMR (DMSO-d6, 400 MHz), chemical shift (ppm): 8.7 (s, 1H), 7.35 (d, J = 9, 1H), 7.25 (m, 3H), 7.15(m, 1H), 6.30 (dd, J = 8.5, 2.5, 2H), 6.05 (d, J = 2.4 Hz, 1H), 3.40 (q, J = 7.0, 4H), 2.30 (s, 3H), 1.15(t, J = 7.0 Hz, 6H).

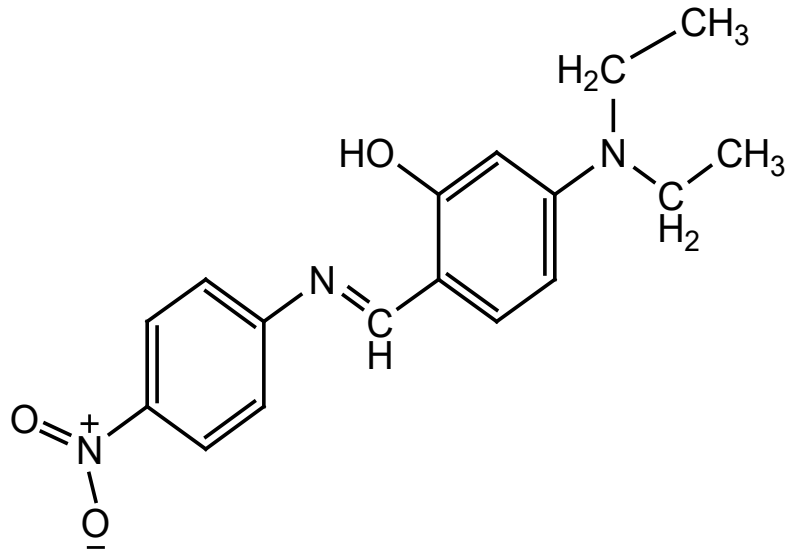

1H-NMR (DMSO-d6, 300 MHz), chemical shift (ppm): 8.56 (s, 1H), 7.85 (d, J = 9.6 Hz,, 1H), 7.275(d, J = 9.2 Hz, 2H), 7.20 (9.6, 2H), 6.68 (br, s, 1H), 6.39 (d, J = 8.4 Hz 1H), 6.09 (s, 1H), 3.49 (q, J = 8.8 Hz, 4H), 1.21 (t, J = 7.6 Hz, 6H)

STRUCTURAL ANALYSIS OF COMPOUNDS (RWT-1and RWT-2)

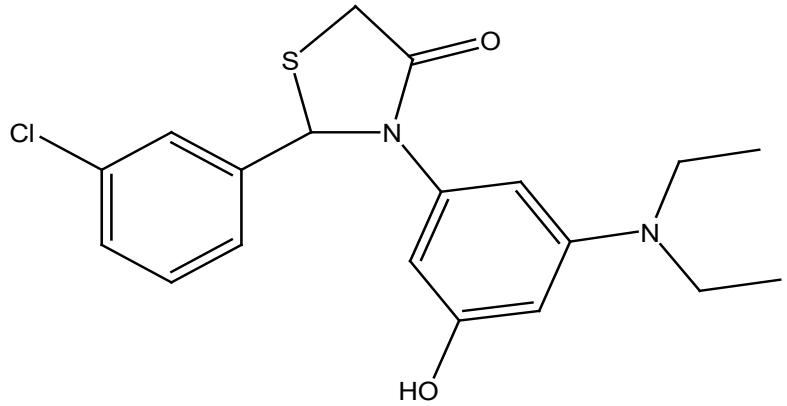

2-(3-chlorophenyl)-3-(3-(diethylamino)-5-hydroxyphenyl)thiazolidin-4-one

1H-NMR (DMSO-d6, 300 MHz), chemical shift (ppm): 7.50 (d, J = 6.8 Hz, 1H),, 7.30 (d, J = 6.0 Hz, 1H), 7.25 (d, J = 2.5 Hz, 1H), 7.20 (dd, J = 6.8, 3.2 Hz, 1H), 7.09 (d, J = 6.01 Hz, 1H), 6.77 (s, 1H), 6.55 (dd, J = 9.6, 1.2 Hz 1H), 6.45 (s, 1H), 6.25 (d, J = 2.8 Hz, 1H), 3.45 (q, J = 6.01 Hz, 4H), 1.15 (t, J = 6.8 Hz, 6H).

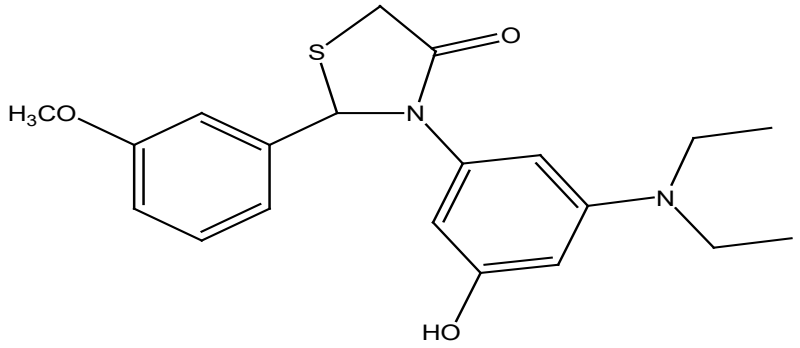

3-(3-(diethylamino)-5-hydroxyphenyl)-2-(3-methoxyphenyl)thiazolidin-4-one

1H-NMR (DMSO-d6, 300 MHz), chemical shift (ppm): 7.29 (d, J = 6.8 Hz, 1H),, 7.10 (d, J = 6.8 Hz, 1H), 6.99 (d, J = 2.8 Hz, 1H), 6.79 (d, J = 6.4 Hz, 1H), 6.75 (dd, J = 8.0, 2.4 Hz, 1H), 6.65 (s, 1H), 6.45 (dd, J = 6.8, 2.4 Hz 1H), 6.25 (s, 1H), 6.12 (d, J = 3.2 Hz, 1H), 3.81 (s, 3H), 3.45 (q, J = 6.0 Hz, 4H), 1.16 (t, J = 7.2 Hz, 6H)

STRUCTURAL ANALYSIS OF COMPOUNDS (RWT-3and RWT-4)

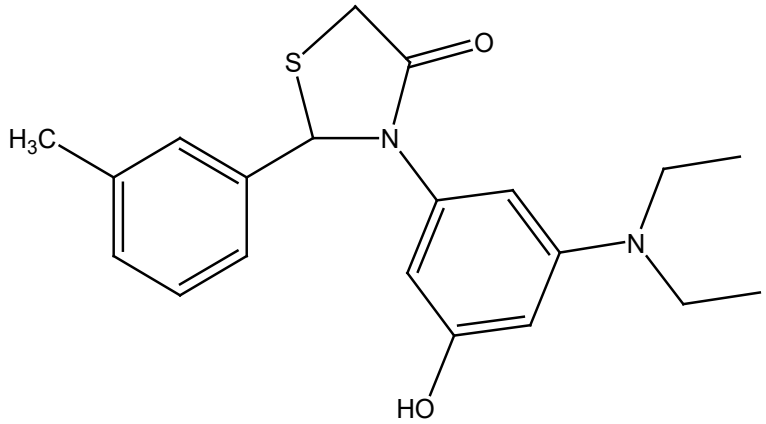

3-(3-(diethylamino)-5-hydroxyphenyl)-2-*m*-tolylthiazolidin-4-one

1H-NMR (DMSO-d6, 300 MHz), chemical shift (ppm): 7.31s (d, J = 6.0 Hz, 1H), 7.27 (dd, J = 6.0, 2.0, Hz, 1H), 7.23 (d, J = 6.4 Hz, 1H), 7.12 (d, J = 6.4 Hz, 1H), 6.90 (d, J = 6.0 Hz, 1H), 6.68 (s, 1H), 6.45 (dd, J = 7.2, 2.0 Hz 1H), 6.35 (d J = 6.4, 1H), 6.27 (d, J = 2.0 Hz, 1H), 3.44 (q, J = 6.0 Hz, 4H), 2.26 (s, 3H), 1.15 (t, J = 7.2 Hz, 6H).

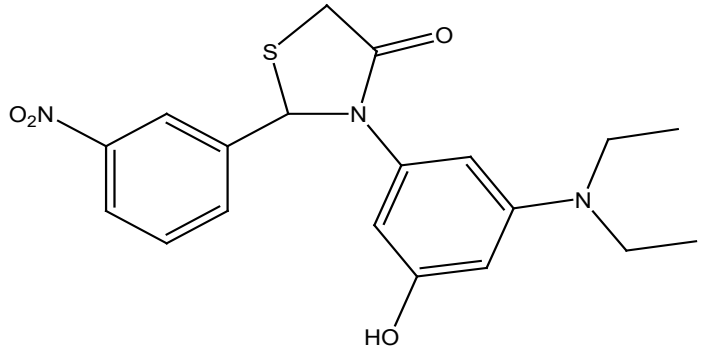

3-(3-(diethylamino)-5-hydroxyphenyl)-2-(3-nitrophenyl)thiazolidin-4-one

1H-NMR (DMSO-d6, 300 MHz), chemical shift (ppm): 8.20 (d, J = 2.4 Hz, 1H),8.15 (dd, J = 6.4, 2.4 Hz, 1H), 7.45 (d, J = 6.0 Hz, 1H), 7.30 (d, J = 6.0 Hz, 1H), 7.15 (d, J = 6.0 Hz, 1H), 6.75 (br s, 1H), 6.45 (dd, J = 6.8, 1.6 Hz 1H), 6.30 (d, J = 6.4 Hz, 1H), 3.45 (q, J = 6.0 Hz, 4H), 1.15 (t, J = 8.0 Hz, 6H)

Biological Assays
Anti-Promastigotes Activity

Compounds	IC_{50}µm/ml *L.Major*	IC_{50}µm/ml *L.tropica*
RW 1	4.55±0.08	22.20±0.01
RW 2	18.75±0.03	36.02±0.06
RW 3	37.18±0.01	37.18±0.04
RW 4	28.17±0.06	41.68±0.02
RW 5	7.49±0.05	9.13±0.01
RW 6	2.17±0.01	10.78±0.08
RW 7	18.98±0.06	34.21±0.09

Anti-Amastigotes Activity

Compounds/ Sample RW-1 TO RW-7	IC_{50} µg/ml
RW 1	09.31±0.07
RW 2	38.80±0.02
RW 3	42.33±0.01
RW 4	12.31±0.02
RW 5	3.30±0.01
RW 6	2.32±0.03
RW 7	10.7±0.09
Standard AMP-B	2.90±0.01

RWT-1 TO RWT-4	Antileishmanial activity (Promastigotes) IC_{50} (µM)
	L. major
RWT 1	8.21 ± 0.02
RWT 2	2.80 ± 0.07
RWT 3	19.55 ± 0.01
RWT 4	1.62 ± 0.03
Amphotericin B (Ve+)	0.60± 0.05
Sodium Stibogluconate (Ve+)	-
DMSO (Ve-)	-

In-Vitro hDHFR Activity

RWT SERIES	hDHFR IC_{50} (Mm)
RWT 1	5.20 ± 0.4
RWT 2	1.05 ± 0.2
RWT 3	8.22 ± 0.2
RWT 4	2.06 ± 0.6
Methotrexate	0.005

Docking Studies Against GAPDH

S#	Ligand Interaction	Docking Score Kcal/mol	A.A residues
1	RW1	-6.595 Kcal/mol	D:VAL219 :- 4.24661 Å A:ARG58 :- 4.88737 Å C:VAL55 :- 4.75663 Å
2	RW2	-5.973 Kcal/mol	:THR54 :- O 3.51045 Å B:ALA299 :- 4.11812 Å D:PRO253 :- 4.29265 Å
3	RW3	-5.769 Kcal/mol	F:GLY11:N :- 3.06137 Å F:ALA90:CB - :UNL1 :- 3.83821 Å F:THR111:CG2 - :UNL1 :- 3.84384 Å
4	RW4	-6.499 Kcal/mol	B:THR197:CB :- 3.6569 Å B:PHE114 :- 5.00251 Å B:ARG12 :- 5.00751 Å B:ILE13 :- 4.82815 Å
6	RW6	-7.136 Kcal/mol	A:ARG249:NH2 :- 3.08736 Å A:ASN335:ND2 :- 3.01541 Å A:ILE13 :- 4.83572 Å
7	RW7	-6.548 Kcal/mol	B:THR54:O :- 2.12709 ÅB:ILE302:CG2 :- 3.85871 Å D:ILE302 :- 4.09779 Å
8	RWT-1	-6.248 Kcal/mol	A:ILE13 :- 3.85763 Å A:MET16 :- 4.49648 Å A:ARG249:NH2:- 4.68972 Å
9	RWT-2	-6.343 Kcal/mol	F:SER165:OG :- 3.18458 Å F:CYS166:SG :- 4.11997 Å F:GLY227:N :- 3.77317 Å
10	RWT-3	-5.753 Kcal/mol	A:TYR339 :- 4.83784 Å A:PRO136 :- 4.05624 Å A:SER165:CB :- 3.49071 Å A:PRO136 :- 4.05624 Å
11	RWT-4	-7.078 Kcal/mol	B:ILE302 :- 5.31046 Å D:ILE302 :- 5.47497 Å D:ILE302 :- 5.45502 Å D:ASN303:ND2 :- 3.82681 Å

3D & 2D Animations

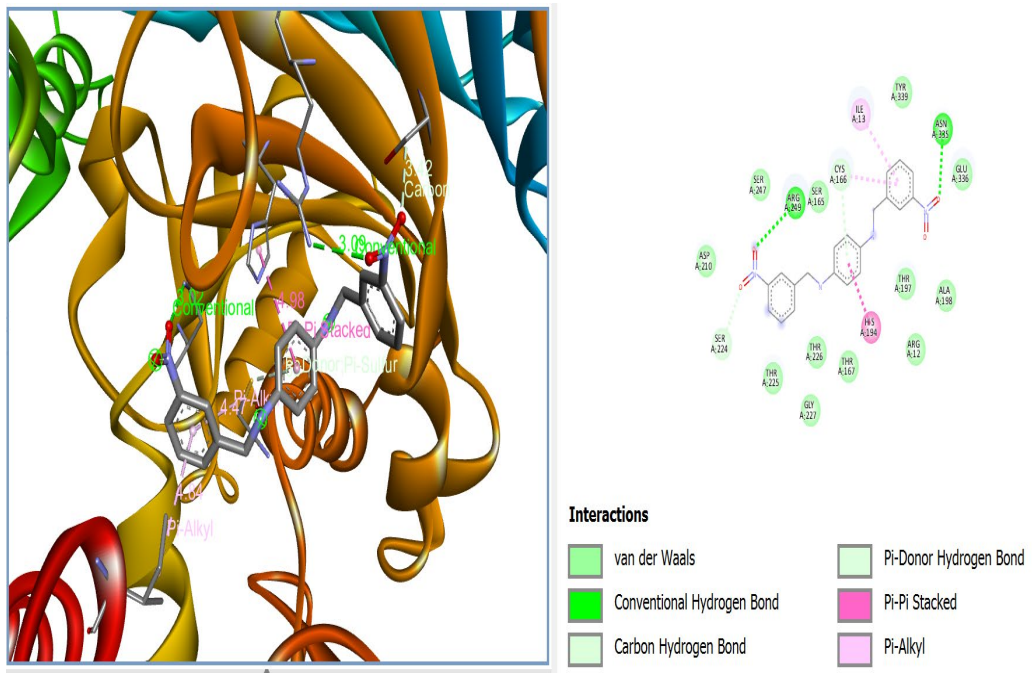

3D & 2D Animation of RWS-6

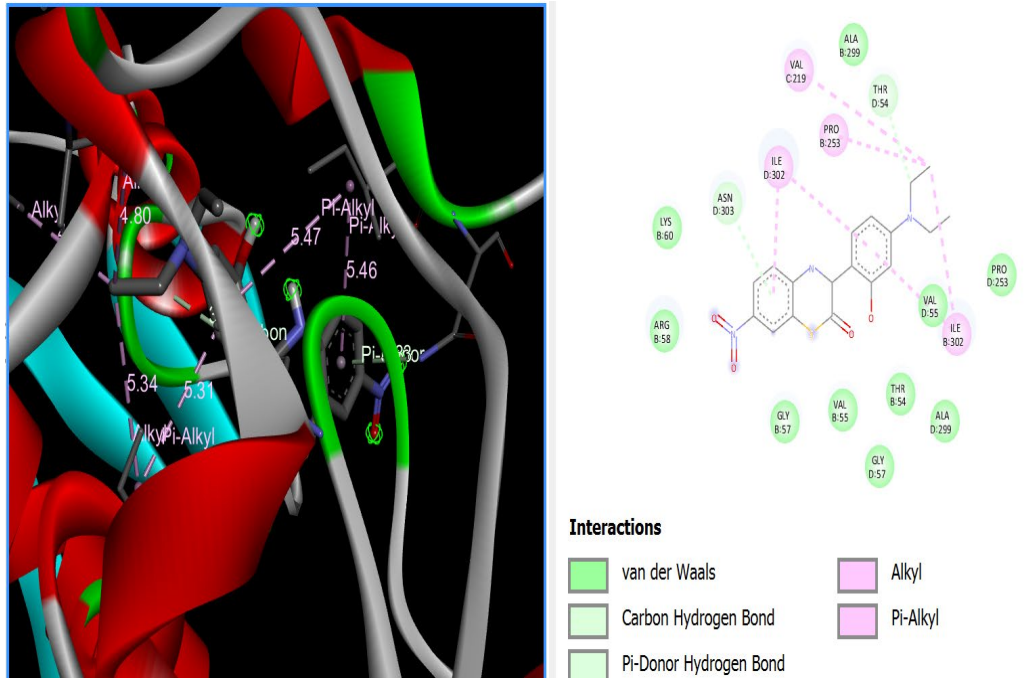

3D & 2D Animation of RWT-4

Docking Studies Against Glutathione Reductase (GR)

S#	Ligand Interaction	Docking Score Kcal/mol	A.A residues
1	RW1	-7.249 Kcal/mol	B:PHE16 :- 5.04289 Å B:TYR46 :- 4.51366 Å B:HIS114 :- 4.62599 Å B:HIS217 :- 4.95413 Å
2	RW2	-6.55 Kcal/mol	B:GLN76:NE2 :- 3.05335 Å B:ARG19:NH1 :- 4.00052 Å
3	RW3	-7.067 Kcal/mol	B:LYS377:O :- 3.47865 Å B:ARG378 :- 4.81603 Å B:LEU248 :- 5.13451 Å
4	RW4	-6.714 Kcal/mol	A:ARG245:NH1 :- 3.15043 Å A:SER294:N :- 2.97508 Å A:GLN295:N :- 2.98656 Å
5	RW5	-7.99 Kcal/mol	B:ARG126:NH2 :- 4.87913 (Electrostatic interaction, not distance-based) B:ARG126:NE :- 3.53118 Å B:PRO276 :-5.04046 Å
6	RW6	-7.639 Kcal/mol	A:ARG19:NH1 :- 2.88743 Å A:ARG19:NH1 :- 4.15982 Å A:CYS14:SG :- 3.58243 Å
7	RW7	-7.14 Kcal/mol	A:CYS240:SG :- 3.88666 Å A:CYS240:SG:B :- 4.03398 Å
8	RWT-1	-7.703 Kcal/mol	B:GLN76:OE1 :- 3.51047 Å B:VAL312:-4.83644Å B:VAL327 :- 5.26163 Å
9	RWT-2	-6.996 Kcal/mol	A:ARG25:C,O;GLU26:N:-4.42103Å A:ALA199 :- 4.30318 Å A:ARG25:CG :- 3.53925 Å
10	RWT-3	-6.652 Kcal/mol	A:LYS170:NZ :- 2.79188 Å A:LYS170:NZ :- 3.46347 Å A:ALA196 :- 5.08722 Å
11	RWT-4	-7.435 Kcal/mol	A:GLU203:OE1:- 2.78049 Å C:ARG25:-4.91251Å C:TYR31 :- 4.8553 Å

3D & 2D Animations

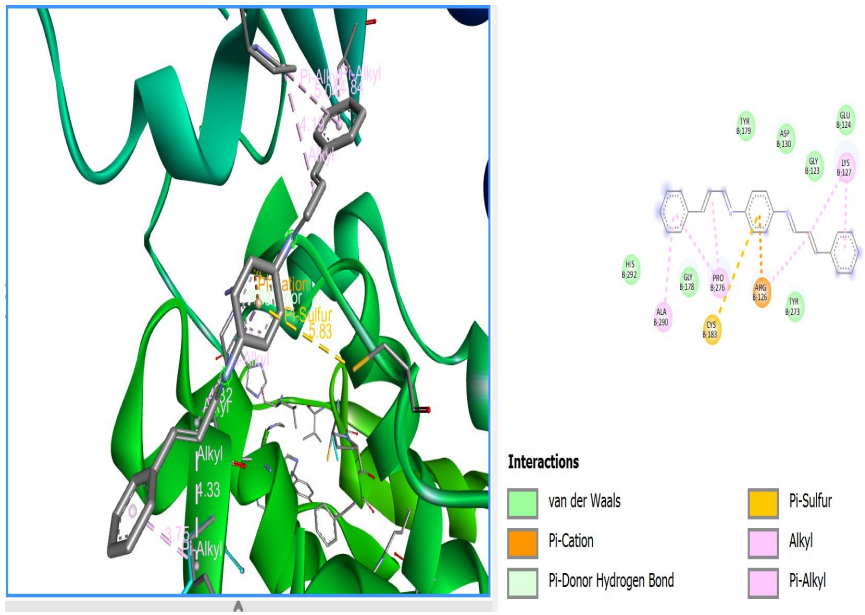

3D & 2D Animation of RWS- 5

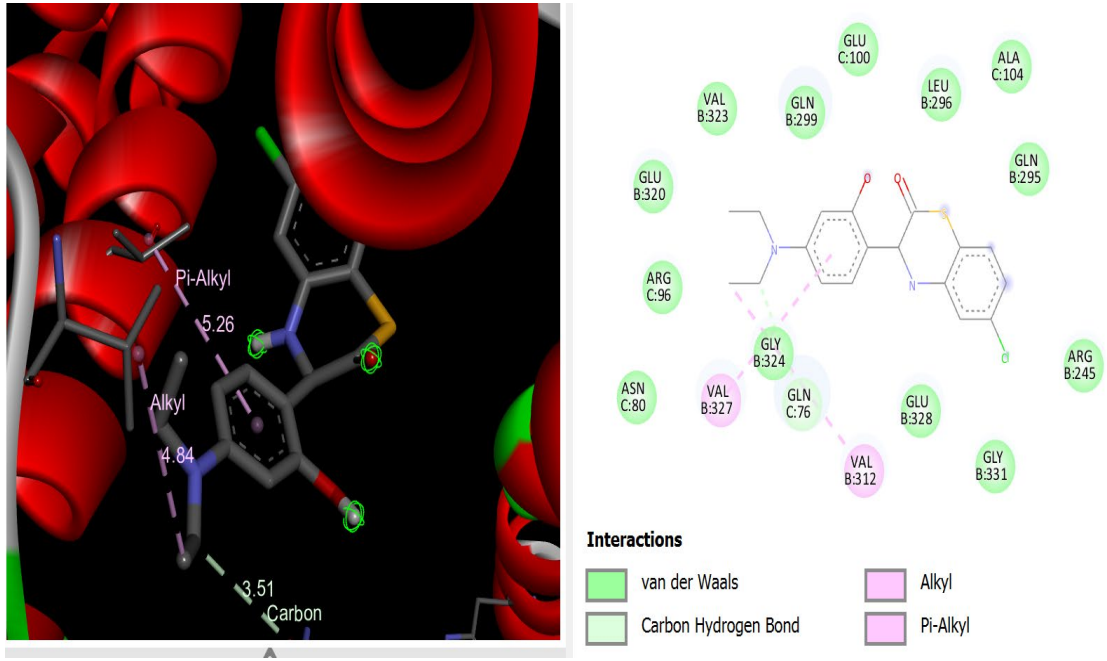

3D & 2D Animation of RWT- 1

Docking Studies Against Trypanothione Reductase (TR)

S#	Ligand Interaction	Docking Score Kcal/mol	A.A residues
1	RW1	-7.242 Kcal/mol	A:ASP327:OD1:- 2.47841 Å A:THR335:OG1 :- 4.19351 Å A:THR160:C,O;GLY161:N :- 4.83861 Å
2	RW2	-7.296 Kcal/mol	A:ALA159:O :- 3.7521 Å A:TYR198 :- 4.40204 Å A:CYS57 :- 5.44134 Å
3	RW3	-6.218 Kcal/mol	A:GLU466:OE2:- 3.5978 Å A:LEU399:- 4.98856 Å A:MET400:- 4.96652 Å B:LYS61:- 4.42365 Å
4	RW4	-6.631 Kcal/mol	B:PRO371 :- 4.7848 Å A:MET400 :- 5.06079 Å A:PRO398 :- 4.99466 Å
5	RW5	-8.91 Kcal/mol	B:ASP327:OD2 :- 3.56051 Å A:THR51:N :- 3.77281 Å A:THR51:OG1 :- 3.79751 Å
6	RW6	-8.14 Kcal/mol	C:- A:SER464:OG :- 3.6661 Å B:LYS61:NZ :- 4.7463 Å B:GLU436:OE2 :-4.47169 Å
7	RW7	-6.987 Kcal/mol	B:GLU466:OE2 :- 2.69263 Å A:LYS61:NZ :- 4.01666 Å B:MET400:N :- 4.16275 Å
8	RWT-1	-6.954 Kcal/mol	A:ARG472:NH2 :- 3.26766 Å B:VAL312 :- 4.83644 Å B:VAL327 :- 5.26163 Å A:SER470:OG :- 4.12776 Å
9	RWT-2	-7.169 Kcal/mol	B:LYS61:NZ :- 3.20472 Å A:PHE396 :- 4.65176 Å
10	RWT-3	-6.6 Kcal/mol	B:ASP432:OD1 :- 4.90234 Å B:PHE367 :- 5.11775 Å A:LEU72 :- 5.29716 Å B:LEU72 :- 5.24336 Å
11	RWT-4	-7.075 Kcal/mol	A:GLU466:OE1 :- 2.00629 Å B:PRO336 :- 5.27474 Å B:ILE339 :- 4.57956 Å

3D & 2D Animations

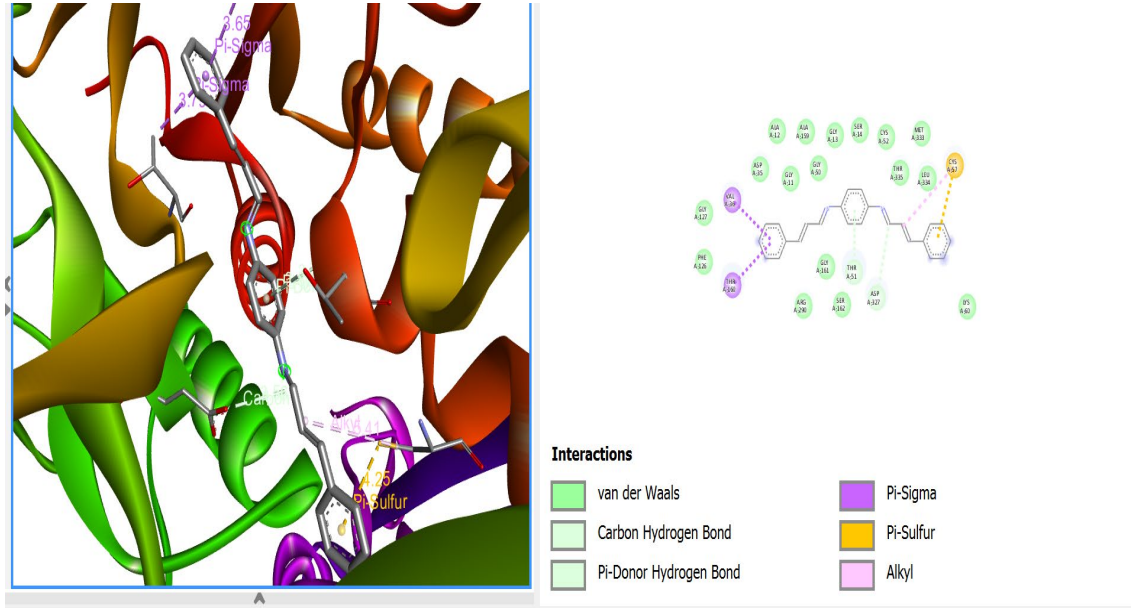

3D & 2D Animation of RWS-5

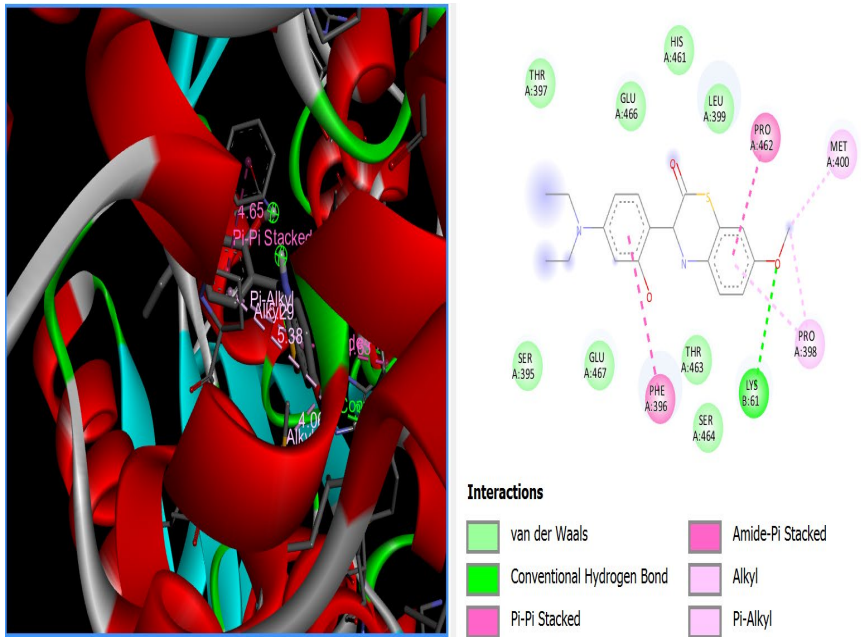

3D & 2D Animation of RWT-2

In Silico Pharmacokinetics Of the Lead Compounds

RWS 1

Molecule	RWS-1
PHARMACOKINETICS (PK)	
GI absorption	High
BBB permeant	Yes
Pgp substrate	No
CYP1A2 inhibitor	Yes
CYP2C19 inhibitor	Yes
CYP2C9 inhibitor	Yes
CYP2D6 inhibitor	Yes
CYP3A4 inhibitor	Yes
log Kp (cm/s)	-5.06
MEDICINAL CHEMISTRY	
PAINS #alerts	0
Brenk #alerts	1
Leadlikeness #violations	1
Synthetic Accessibility	2.64

RWS 5

Molecule	RWS-5
PHARMACOKINETICS (PK)	
GI absorption	Low
BBB permeant	No
Pgp substrate	Yes
CYP1A2 inhibitor	No
CYP2C19 inhibitor	Yes
CYP2C9 inhibitor	Yes
CYP2D6 inhibitor	No
CYP3A4 inhibitor	No
log Kp (cm/s)	-5.62
MEDICINAL CHEMISTRY	
PAINS #alerts	0
Brenk #alerts	3
Leadlikeness #violations	2
Synthetic Accessibility	3.04

In Silico Pharmacokinetic Studies Of the lead Compounds (Continued)

RWT 1

Molecule	RWT-1
PHARMACOKINETICS (PK)	
GI absorption	High
BBB permeant	No
Pgp substrate	No
CYP1A2 inhibitor	Yes
CYP2C19 inhibitor	Yes
CYP2C9 inhibitor	Yes
CYP2D6 inhibitor	Yes
CYP3A4 inhibitor	Yes
log Kp (cm/s)	-5.08
MEDICINAL CHEMISTRY	
PAINS alerts	2
Brenk alerts	1
Leadlikeness violations	2
Synthetic Accessibility	3.59

RWT 2

Molecule	RWT-2
PHARMACOKINETICS (PK)	
GI absorption	High
BBB permeant	No
Pgp substrate	No
CYP1A2 inhibitor	Yes
CYP2C19 inhibitor	Yes
CYP2C9 inhibitor	Yes
CYP2D6 inhibitor	Yes
CYP3A4 inhibitor	Yes
log Kp (cm/s)	-5.53
MEDICINAL CHEMISTRY	
PAINS alerts	3
Brenk alerts	1
Leadlikeness violations	2
Synthetic Accessibility	3.82

In Silico Toxicology Studies Of the lead Compounds

RWS 1

Predicted LD50	1000mg/kg
Predicted Toxicology class	4
Organ Toxicity	Cardiotoxicity cardio (Inactive) 0.63 Respiratory toxicity respi (Active) 0.81 Neurotoxicity neuro (Active) 0.73
Toxicity end point	Ecotoxicity eco (Active) 0.75 Clinical toxicity clinical (Active) 0.51 Nutritional toxicity nutri (Inactive) 0.54
Metabolism	Cytochrome CYP2C9 CYP2C9 (Active) 0.50 Cytochrome CYP2D6 CYP2D6 (Active) 0.84 Cytochrome CYP3A4 CYP3A4 (Inactive) 0.86

RWS 5

Predicted LD50	350mg/kg
Predicted Toxicology class	4
Organ Toxicity	Respiratory toxicity respi (Active) 0.64 Neurotoxicity neuro (Active) 0.64 Cardiotoxicity cardio (Inactive) 0.74
Toxicity end point	BBB-barrier bbb (Active) 0.93 Ecotoxicity eco (Active) 0.90 Clinical toxicity clinical (Inactive) 0.61
Metabolism	Cytochrome CYP1A2 CYP1A2 (Active) 0.59 Cytochrome CYP2C19 CYP2C19 (Active) 0.70 Cytochrome CYP2C9 CYP2C9 (Inactive) 0.63

In Silico Toxicology Studies Of the lead Compounds (Continued)

RWT 1

Predicted LD50	500mg/kg
Predicted Toxicology class	4
Organ Toxicity	Respiratory respi (Active) 0.89 Neurotoxicity neuro (Active) 0.56 Cardiotoxicity cardio (Inactive) 0.72
Toxicity end point	Immunotoxicity immuno (Active) 0.98 Mutagenicity mutagen (Active) 0.55 Cytotoxicity cyto (Inactive) 0.57
Metabolism	Cytochrome CYP2D6 CYP2D6 (Active) 0.61 Cytochrome CYP3A4 CYP3A4 (Inactive) 0.66 Cytochrome CYP2E1 CYP2E1 (Inactive) 0.99

RWT 2

Predicted LD50	560mg/kg
Predicted Toxicology class	4
Organ Toxicity	Neurotoxicity neuro (Active) 0.56 Nephrotoxicity nephro (Inactive) 0.59 Respiratory toxicity respi (Active) 0.90
Toxicity end point	Immunotoxicity immuno (Active) 0.95 Mutagenicity mutagen (Active) 0.54 Cytotoxicity cyto (Inactive) 0.55
Metabolism	Cytochrome CYP2D6 CYP2D6 (Active) 0.62 Cytochrome CYP3A4 CYP3A4 (Inactive) 0.76 Cytochrome CYP2E1 CYP2E1 (Inactive) 0.99

SAR Analysis of Lead Compounds

RWS-1

The hydroxyl group on the phenol ring may participate in hydrogen bonding with enzyme residues, stabilizing the compound-enzyme complex.

The 3-chlorophenyl group is crucial for activity, possibly due to its electron-withdrawing properties, which may enhance binding affinity to the enzyme by forming strong interactions with active site residues.

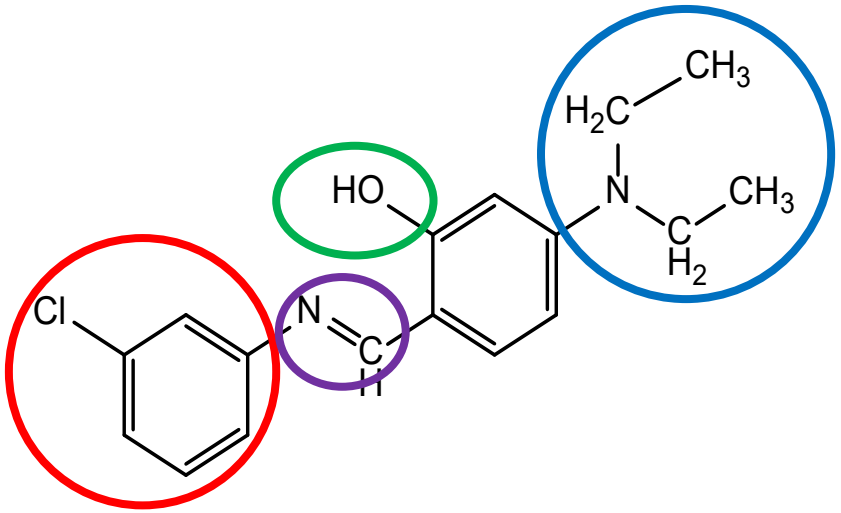

The presence of the diethylamino group at the para position of the phenol ring plays a significant role in enhancing the anti-Leishmanial activity. This group likely increases lipophilicity, facilitating better cellular uptake and interaction with the target enzyme.

The imine linkage (C=N) connects the aromatic systems, providing rigidity to the molecule, which could be important for optimal positioning within the enzyme's active site.

SAR Analysis of Lead Compounds

RWS-5

The phenyl rings at both ends of the molecule can engage in π-π stacking interactions with aromatic residues within the enzyme, contributing to the stabilization of the compound-enzyme complex.

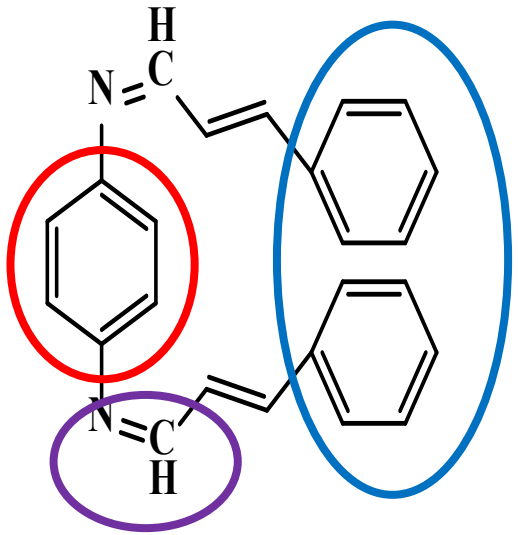

The imine linkage (C=N) connects the aromatic systems, providing rigidity to the molecule, which could be important for optimal positioning within the enzyme's active site.

The 1,4-phenylene core provides a planar structure that may facilitate intercalation into the enzyme's active site.- The presence of the bis(3-phenylprop-2-en-1-imine) groups on either side of the phenylene ring is crucial for the compound's activity. These groups increase the overall hydrophobicity and may enhance interactions with hydrophobic pockets of the enzyme.

SAR Analysis of Lead Compounds

RWT-1

The thiazolidin-4-one ring is a crucial scaffold for activity, providing a rigid, three-dimensional structure that fits well within the enzyme's active site.

The 3-chlorophenyl group enhances binding affinity through potential hydrophobic interactions and possibly through halogen bonding with enzyme residues.

The diethylamino group at the para position of the phenol ring enhances the compound's lipophilicity and may improve its cellular uptake and binding to the enzyme.

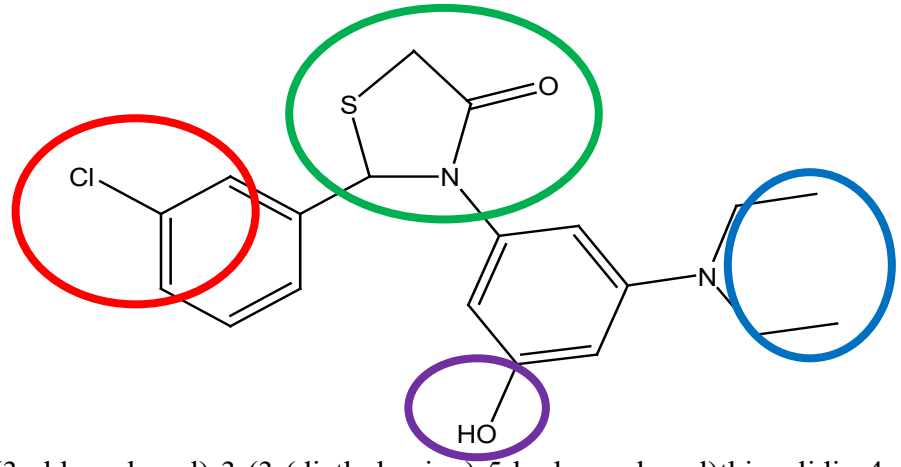

2-(3-chlorophenyl)-3-(3-(diethylamino)-5-hydroxyphenyl)thiazolidin-4-one

The hydroxyl group on the phenol ring is likely involved in hydrogen bonding with active site residues, contributing to the stabilization of the enzyme-inhibitor complex.

SAR Analysis of Lead Compounds

RWT-2

The thiazolidin-4-one ring is a crucial scaffold for activity, providing a rigid, three-dimensional structure that fits well within the enzyme's active site.

The 3-methoxyphenyl group contributes to the compound's overall hydrophobic character and may engage in hydrophobic interactions within the enzyme's active site.

The diethylamino group at the para position of the phenol ring enhances the compound's lipophilicity and may improve its cellular uptake and binding to the enzyme.

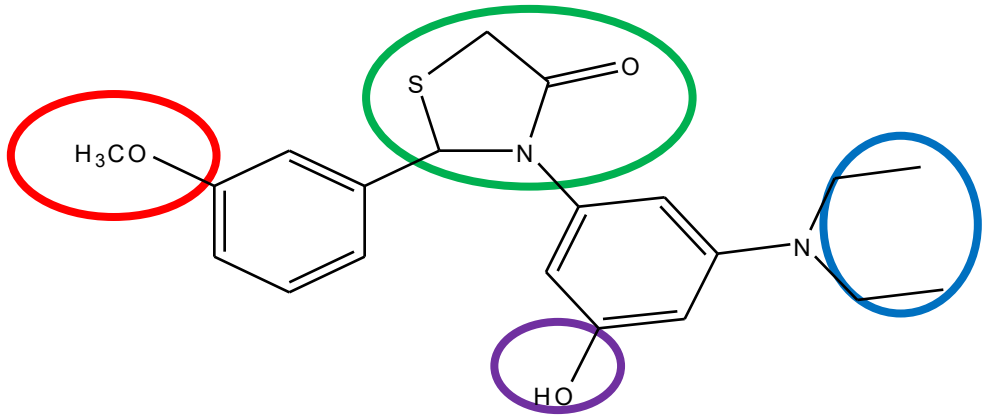

3-(3-(diethylamino)-5-hydroxyphenyl)-2-(3-methoxyphenyl)thiazolidin-4-one

The hydroxyl group on the phenol ring is likely involved in hydrogen bonding with active site residues, contributing to the stabilization of the enzyme-inhibitor complex.

Discussion

The study focused on the synthesis, characterization, and biological evaluation of Schiff bases and thiazolidine derivatives as potential anti-Leishmanial agents. Specifically, six Schiff bases (RWS-1 to RWS-7) and four thiazolidine derivatives (RWT-1 to RWT-4) were synthesized and evaluated. The synthesized compounds were subjected to various in vitro and in silico assays to determine their efficacy against Leishmania parasites. Among these, RWS-5, RWS-6, RWS-1, RWT-4, RWT-1, and RWT-2 demonstrated significant activity, with RWS-5 showing the highest binding affinity (-7.91 Kcal/mol) and RWT-4 displaying a strong interaction (-7.18 Kcal/mol) in docking studies.

The *in vitro* IC_{50} values revealed that compounds such as RWS-1 (4.55±0.08 μM), RWS-5 (7.49±0.05 μM), and RWT-1 (1.16±0.02 μM) exhibited notable anti-Leishmanial activity. These results were consistent with the *in silico* docking scores, suggesting a good correlation between computational predictions and experimental outcomes. The integration of docking studies helped identify key interactions at the molecular level, thereby providing insights into the binding mechanisms of these compounds with Leishmania enzymes.

Discussion (Continued)

The structure-activity relationship (SAR) analysis revealed critical structural features contributing to the anti-Leishmanial activity. For instance, the presence of the nitro group in RWS-6 and RWT-4 was found to enhance binding affinity and biological activity. Similarly, the diethylamino group in RWS-1 and the chloro group in RWT-1 were pivotal in increasing the compounds' potency. These findings underscore the importance of specific substituents in modulating the biological activity of Schiff bases and thiazolidine derivatives.

The docking studies highlighted significant binding interactions of the compounds with key residues of Leishmania enzymes. Schiff bases such as RWS-5 and RWS-6 interacted with residues like ARG58, ILE302, and VAL55, while thiazolidine derivatives like RWT-4 and RWT-1 showed strong interactions with ARG249, CYS166, and TYR339. These interactions suggest that the compounds can effectively inhibit enzyme activity, thereby impairing the parasite's survival and proliferation.

Discussion (Continued)

The identified interactions and binding affinities suggest potential mechanisms of action for the most active compounds. RWS-5 and RWT-4, for example, may inhibit critical metabolic pathways in Leishmania by binding to and inhibiting key enzymes involved in parasite metabolism. The strong binding affinities and specific interactions with enzyme residues highlight the potential of these compounds to disrupt vital biological processes in the parasite, leading to its eradication.

Future research should focus on further optimizing the structures of these lead compounds to enhance their anti-Leishmanial activity and reduce potential toxicity. Additionally, in vivo studies are necessary to confirm the efficacy and safety of these compounds in animal models. The promising results from this study provide a solid foundation for the development of novel anti-Leishmanial agents, contributing to the ongoing efforts to combat this debilitating disease. Continued exploration of Schiff bases and thiazolidine derivatives could yield potent therapeutics with improved pharmacokinetic and pharmacodynamic properties.

Conclusion

Leishmaniasis, caused by Leishmania protozoa, remains a significant global health challenge primarily affecting tropical and subtropical regions. Current treatments are inadequate, characterized by limited efficacy, severe side effects, and increasing drug resistance, underscoring the urgent need for new therapeutic options. This study synthesized and evaluated seven Schiff bases (RWS-1 to RWS-7) and four Thiazolidine derivatives (RWT-1 to RWT-4) for their potential against Leishmania species. Promisingly, compounds like RWS-5 and RWS-6 showed potent anti-promastigote and anti-amastigote activities against both *L. major* and *L. tropica*, while RWT-1 exhibited strong efficacy against *L. major*. Conversely, RWS-3 and RWT-3 demonstrated lower activity levels in these assays.

Additionally, the synthesized compounds were assessed for their inhibitory effects on human dihydrofolate reductase (hDHFR) and Leishmania dihydrofolate reductase, with RWT-2 proving most effective among the Thiazolidine derivatives. In silico molecular docking studies targeted key Leishmania enzymes, revealing that RWS-5, RWS-6, and RWS-1 exhibited the highest binding affinities for enzymes crucial to parasite metabolism and survival. Similarly, RWT-4 emerged as the most promising Thiazolidine derivative in these simulations.

Conclusion

Schiff bases are valued in medicinal chemistry for their versatility and structural influence on biological activities, attributed in part to their azomethine group (-C=N-). Thiazolidine derivatives, featuring a thiazolidine ring, possess inherent bioactive potential due to interactions facilitated by sulfur and nitrogen atoms within their structure. These compounds are recognized for their broad pharmacological profiles, encompassing antimicrobial and anti-inflammatory properties, which underscore their suitability for targeted drug development against leishmaniasis.

In conclusion, this study underscores the therapeutic promise of Schiff bases and Thiazolidine derivatives against leishmaniasis, highlighting specific compounds like RWS-5, RWS-6, RWT-1, and RWT-4 for further investigation and development as effective treatments for this debilitating parasitic disease.

Future Prospectives

Future studies need to be carried out for those potential compounds to further evaluate their therapeutic potential. These studies should include:

1. Pharmacokinetic profile studies
2. Pharmacodynamic profile studies
3. In vivo studies on mice and toxicity studies

Acknowledgment

- **Dr. Yasser MSA Al-kahraman,** Associate Professor, Department of Pharmacy, Comsats University Islamabad, Abbottabad campus
- **Dr. Muhammad Hasham Bin Asad,** Assistant Professor, Department of Pharmacy, Comsats University Islamabad, Abbottabad campus
- **Prof. Dr. Abdul Jabbar Shah,** Chairman , Department of Pharmacy, Comsats University Islamabad, Abbottabad campus
- **Prof. Dr. Abdul Mannan,** Head of Department, Department of Pharmacy, Comsats University Islamabad, Abbottabad campus
- **Dr. Taous Khan** Professor, Department of Pharmacy, Comsats University Islamabad, Abbottabad campus

References

Ahmed, S., & Bhatti, A. (2020). Schiff base complexes in catalysis: An overview. *Catalysis Reviews, 62*(3), 274-295.

Baran, T., & Yüce, S. (2021). Schiff base metal complexes as catalysts in organic transformations. *Journal of Molecular Catalysis A: Chemical, 406*, 136-147.

Chen, X., Zhang, Y., & Liu, Y. (2019). Thiazolidine derivatives as potent antidiabetic agents. *Medicinal Chemistry Research, 28*(5), 865-872.

Das, S., & Mukherjee, S. (2020). Thiazolidines as anti-inflammatory agents: A comprehensive review. *Journal of Medicinal Chemistry, 63*(14), 7862-7875.

Edwards, S., & Brown, P. (2021). Novel thiazolidine derivatives in the treatment of infectious diseases. *Future Medicinal Chemistry, 13*(7), 557-570.

Gajare, R. K., & Bhat, M. A. (2021). Synthesis and applications of Schiff base complexes in medicinal chemistry. *Journal of Molecular Structure, 1245*, 131104.

Halder, S. K., & Roy, S. (2019). Leishmanial modulation of host immune response: Mechanisms and therapeutic opportunities. *Journal of Immunology Research, 2019*, 345721.

Jadhav, P., & Desai, S. (2019). Synthesis and pharmacological activities of thiazolidine derivatives. *European Journal of Medicinal Chemistry, 166*, 360-377.

Jain, S., & Sharma, R. (2019). Structural elucidation and biological activities of Schiff bases. *Chemical Biology & Drug Design, 94*(5), 1455-1468.

Kamble, V. B., & Rao, B. (2021). Antimicrobial potential of thiazolidine-4-one derivatives: A review. *Microbial Pathogenesis, 152*, 104673.

References

Kumar, R., & Nylec, N. (2020). Molecular mechanisms of drug resistance in Leishmania species. *Journal of Medical Microbiology, 69*(4), 502-510.

Liu, Y., & Tang, J. (2021). Design and synthesis of novel thiazolidine derivatives with anticancer activity. *Journal of Chemical Sciences, 133*, 68.

Mahmoudzadeh, H., & Mohammadi, M. (2018). Clinical manifestations and management of cutaneous leishmaniasis in Iran. *Iranian Journal of Parasitology, 13*(3), 356-368.

Oliveira, A. L., & Oliveira, M. (2020). Thiazolidine derivatives in medicinal chemistry: An overview. *Journal of Advanced Research, 24*, 145-161.

Patel, M., & Patel, R. (2021). Schiff base metal complexes: Synthesis, characterization, and biological activity. *Journal of Coordination Chemistry, 74*(10), 1764-1782.

Qureshi, S., & Jabeen, F. (2020). Thiazolidine derivatives in the development of anti-inflammatory agents. *Journal of Chemical Sciences, 132*, 58.

Rao, K., & Patil, R. (2019). Thiazolidine analogs as potential therapeutic agents for diabetes and cancer. *Mini Reviews in Medicinal Chemistry, 19*(6), 453-468.

Singh, O. P., & Sundar, S. (2019). Strategies for treatment of visceral leishmaniasis: Current approaches and future directions. *Journal of Infection and Chemotherapy, 25*(8), 577-590.

Srivastava, A., & Basu, R. (2020). Leishmaniasis: Recent developments in epidemiology and control measures. *Clinical Epidemiology and Global Health, 8*(3), 965-973.

Yasinzai, M. M., & Khan, M. (2020). Leishmania and immunomodulation: Implications for novel therapeutics. *Journal of Infection and Public Health, 13*(4), 584-590.


Thank you